2006-03-15

Unresolved Problems Involving the Hydrogeology and Sequence Stratigraphy of the Wasatch Plateau based on Mapping of the Wattis 7.5 Minute Quadrangle, Carbon and Emery Counties, Utah: Insights Gained from a New Geologic Map

David O. Alderks
Brigham Young University - Provo

UNRESOLVED PROBLEMS INVOLVING THE HYDROGEOLOGY AND SEQUENCE STRATIGRAPHY OF THE WASATCH PLATEAU BASED ON MAPPING OF THE WATTIS 7.5 MINUTE QUADRANGLE, CARBON AND EMERY COUNTIES, UTAH: INSIGHTS GAINED FROM A NEW GEOLOGIC MAP

by

David Otto Alderks

A thesis submitted to the faculty of

Brigham Young University

in partial fulfillment of the requirements for the degree of

Master of Science

Department of Geology

Brigham Young University

April 2006

BRIGHAM YOUNG UNIVERSITY

GRADUATE COMMITTEE APPROVAL

of a thesis submitted by

David Otto Alderks

This thesis has been read by each member of the following graduate committee and by majority vote has been found to be satisfactory.

Date	Stephen T. Nelson, Chair
Date	Thomas H. Morris
Date	Barry Bickmore

BRIGHAM YOUNG UNIVERSITY

As chair of the candidate's graduate committee, I have read the thesis of Daniel H. Martin in its final form and have found that (1) its format, citations, and bibliographical style are consistent and acceptable and fulfill the university and department style requirements; (2) its illustrative materials including figures, tables, and charts are in place; and (3) the final manuscript is satisfactory to the graduate committee and is ready for submission to the university library.

_____ _____

Date

Stephen T. Nelson
Chair, Graduate Committee

Accepted for the Department

_____

Bart J. Kowallis
Graduate Coordinator

Accepted for the College

_____

Tom Sederberg
Dean, College of Physical and
Mathematical Sciences

ABSTRACT

UNRESOLVED PROBLEMS INVOLVING THE HYDROGEOLOGY AND SEQUENCE STRATIGRAPHY OF THE WASATCH PLATEAU BASED ON MAPPING OF THE WATTIS 7.5 MINUTE QUADRANGLE, CARBON AND EMERY COUNTIES, UTAH

David O. Alderks

Department of Geology

Master of Science

The Wattis 7.5 Minute Quadrangle is located in central Utah, in the transition zone between the Basin and Range province and the Colorado plateau. Two small grabens, located in the quadrangle, are the easternmost evidence of Basin and Range faulting. Sedimentary units exposed are mainly Cretaceous in age and deposited in the Western Cretaceous Interior Seaway. This area is of economical importance due to its large coal deposits, coal bed methane, and groundwater.

The Wattis Quadrangle provided an ideal opportunity to test, at a small scale, the applicability of a new groundwater model for stratified mountainous terranes. Water samples had ^{14}C ages ranging from modern to 10,000 ± 500 years. Stable isotopes of oxygen and hydrogen showed that recharged precipitation fell when climate conditions were close to modern, or slightly colder. Three groundwater systems consist of one shallow groundwater system in the North Horn Formation, and two deeper aquifers located in the Blackhawk Formation and the Star Point Sandstone. Water in the North Horn Formation is modern, whereas the Blackhawk Formation and Star Point Sandstone

waters are mixed systems, having tritium concentrations between 3 and 4 T.U., and ^{14}C ages between 7,000 and 10,000 years. Geochemical modeling shows that there are no plausible reaction paths to evolve the North Horn Formation waters into waters contained in underlying units. Thus, water entering the top of the plateau does not flow through the stratified rocks to exit at its base. Instead, the waters represent discrete perched systems at various stratigraphic levels.

The Star Point Sandstone has three parasequences with a single sequence boundary. The deposits show normal marine conditions containing lower shoreface biota of *Skolithos* and *Ophiomorpha* overlain by middle shoreface sedimentary structures. The Star Point Sandstone deltaic parasequences likely prograded into the basin during pulses of thrusting from the Sevier Orogeny.

The Emery Sandstone Member of the Mancos Formation contains three parasequences all located in the lower shoreface, and also exhibits the normal marine biota of *Skolithos* and *Ophiomorpha*. The Emery Sandstone reflects density currents caused by major storm events, including Bauma C and D depositional structures. Thick sandstone bodies are restricted to paleochannels.

PREFACE

The thesis is a synthesis of four activities: mapping, a description of coal and coalbed methane deposits, hydrogeological investigations, and sequence stratigraphic studies, where mapping was conducted in support of the other activites.

This thesis is divided into several chapters. Chapter 1 contains an overview of the preparation of the geologic map, a summary of previous research conducted in the area, a description of map units, and a discussion of geological structures in the area. Chapter 2 examines at the hydrogeology of the Wattis Quadrangle in the context of the conceptual model of Mayo et al. (2004). Chapter 3 discusses the sequence stratigraphy of the Emery and Star Point Sandstones, whereas Chapter 4 catalogs important economic deposits in and near the Wattis Quadrangle.

Two plates are included for the geological map, unit descriptions, and cross sections of the Wattis UT 7.5' quadrangle. Along with four appendices containing the hydrological data collected for this study.

ACKNOWLEDGEMENTS

First of all I would like to thank Dr. Stephen Nelson for his support and encouragement that he has given me. I would also like to thank Drs. Thomas Morris and Dr. Alan Mayo for their support and guidance. I would also like to thank David Tingey for his patience with me during the lab work, for his teaching ability, and solving the difficulties that arose during lab analysis. Thanks also owed to Dr. Barry Bickmore for filling in for my thesis defense. I would also like to thank Jay Wood and Katie Anderson for their help with the lab work for water samples, Matt Young for all the countless days he helped with mapping and patience in extricating us from snow drifts. Matt's wife was kind for letting him spend so much time in the field. Thanks go to Andy Stanton for his assistance collecting water samples, volunteering to be a pack animal, and for the use of his digital camera. Dan Martin kindly spent some of his weekends in the field working on sequence stratigraphy of the Star Point Sandstone, and for the use of his digital camera. I would also like to thank Peter Alderks for his help in collecting samples and watching me get stuck in the mud trying to get the samples out.

Special thanks go to Fred and Marge Alderks for the financial help that they gave to me during the graduate years. I would also like to thank my parents for support, by finding me a Jeep, and especially for my father on his reviewing of my project and offering suggestions.

Also thanks go to the many unmentioned graduate student at Brigham Young University for their friendship while we were here together.

TABLE OF CONTENTS

LIST OF FIGURES

TABLE OF TABLES

INTRODUCTION

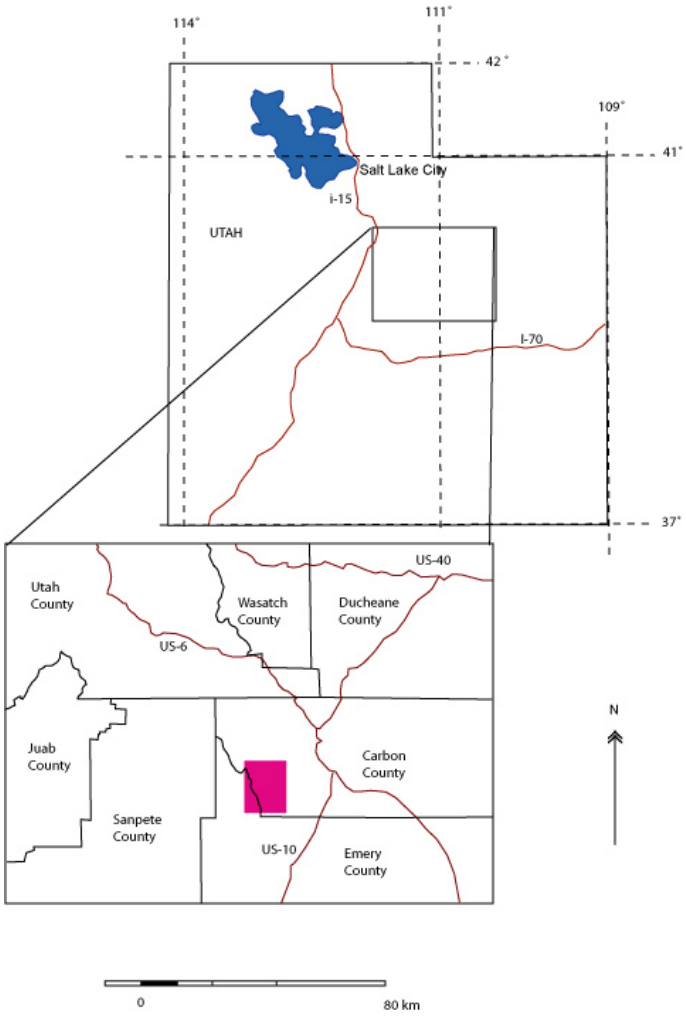

Figure 1. Location of Wattis Quadrangle in Central Utah. Quadrangle shown in red box is located on the western boundary of Carbon and Emery Counties, Utah.

This thesis deals with four geological aspects of the Wattis 7.5 Minute Quadrangle, located in Emery and Carbon Counties, in Central Utah (Figure 1). They are: 1) a geological map produced at the 1:24,000 scale, 2) the hydrogeology of the quadrangle focused on the Wasatch plateau, 3) the sequence stratigraphy of the Star Point and Emery Sandstones, and 4) the economic potential of the quadrangle. Each of these aspects will be discussed in detail separately.

Geological Setting

Cretaceous Period

The Cretaceous Period was eventful in Utah. The Sevier Orogeny had been active since Late Jurassic time (Hintze, 1988). Sevier orogenic thrust sheets exploited bedding

planes in thick Paleozoic and Mesozoic sediments by propagating thrust faults along weaker bedding planes. As a thin-skinned tectonic events occurred (USGS, 2005), a foreland basin developed in eastern Utah ahead of eastward vergent thrust faults, and an epicontinental seaway to encroached from the Arctic Ocean to the Gulf of Mexico (Hintze 1988, Van Wagoner 1988). Sediment was shed to the east from the orogeny and was deposited in the deepening foreland basin, resulting in an interfingering of terrestrial and marine sediments (Hintze 1988, Spieker 1931, Spieker 1949, Carrol 1987, Elder 1994; Figure 2).

These interfingering relationships can be seen in the Emery Sandstone and Star Point Sandstones of the Mancos Shale. During the Middle to Late Campainian, tectonism switched from the thin-skinned Sevier thrusts to the thick-skinned deformation involving deep seated basement blocks of the Laramide Orogeny (Elder 1994). At this time, the area of most rapid subsidence migrated eastward into Colorado (Lawton 1994, Cross, 1988). The migration of the deepest part of the basin to the east allowed for the development of a large prograding wedge of sediment eastward from the thrust sheets. This wedge first consisted of coastal plain, beach sands, spits and barrier island deposits, with lagoons and swamps behind the beaches (Elder 1994, Flores 1984). This changed the sediments deposited in the Wattis Quadrangle from marine to terrigenous deposits. As the clastic wedge continued to prograde eastward, the area of the Wattis Quadrangle changed from this coastal environment to a fluvial-dominated environment as the large braided river system of the Castlegate Formation, transported sediments to large deltas near the Utah-Colorado border (Carrol 1987, Van Wagoner 1995).

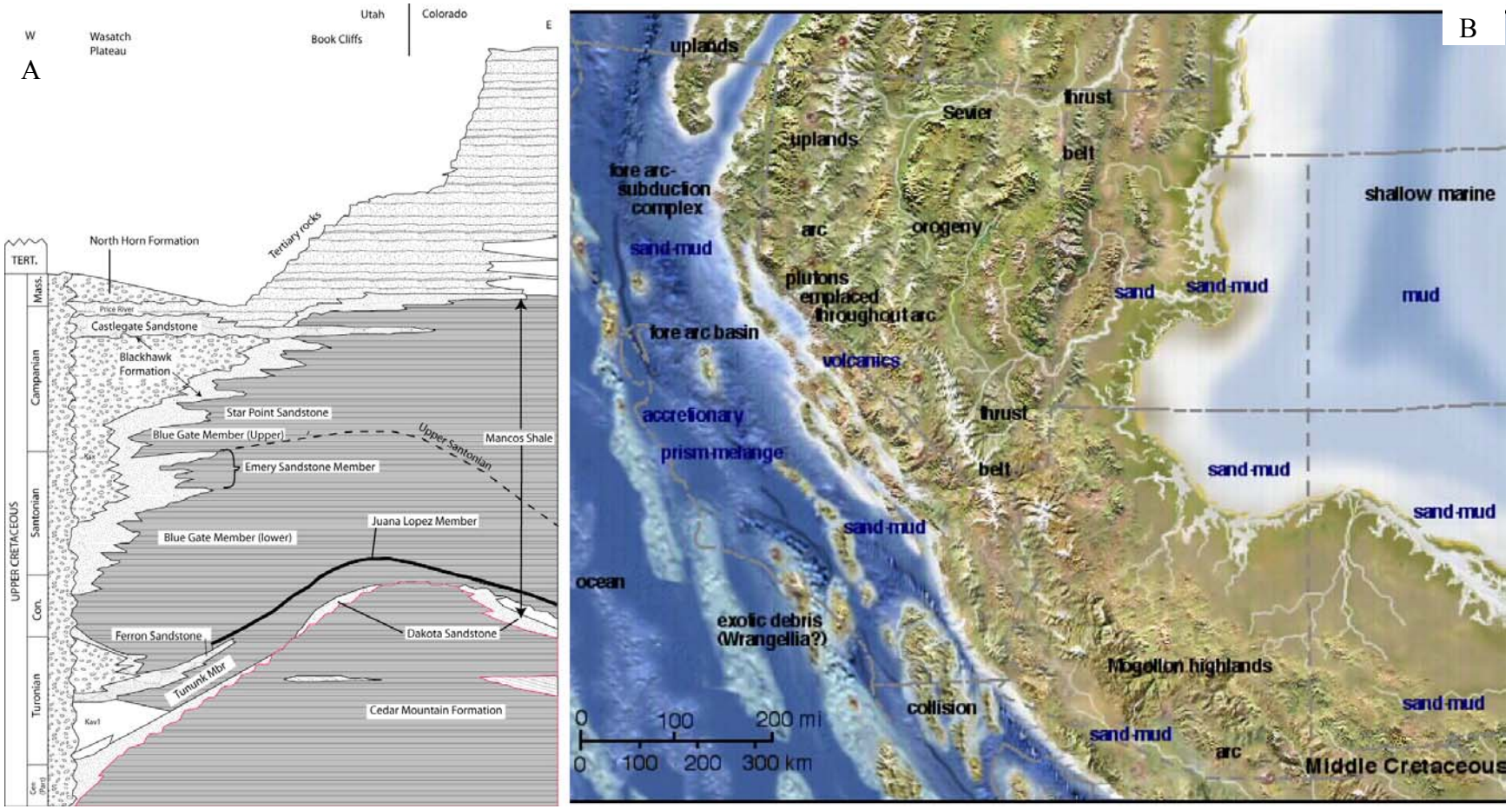

Figure 2. A: West-east lithostratigraphic cross section of Cretaceous rocks from central Utah to the Colorado state line. Cross section shows the interfingering of terrigenous and marine sediments in the western part of the foreland basin of the Sevier orogen. Terrigenous sediments prograde to the eas. Modified from Dyman, 1990.B: Paleogeography of Utah and the western United States during the middle Cretaceous Period. Box marks the general location of the study area. Modified from Blakey, 2005.

As the Laramide Orogeny continued, the foreland basin was evetually broken up into several smaller intermontaine basins (Elder 1994), which reorganized the transport of sediment from the east to northeast along with the development of intermontane lakes (Elder 1994, Van Wagoner 1995).

Tertiary Period

During the early part of the Cenozoic Era, Lake Flagstaff was established and persisted in the area (UGS 2005) accompanied by the deposition of mudstones, siltstones, and marls. Limestones, which were once presumably present have subsequently been eroded away, and can be found to the west and north of the Wattis Quadrangle about 25 km away. Between 25 and 8 Ma, uplift of the Colorado Plateau began accompanied with localized igneous represented by the intrusion of minette dikes (Tingey 1989). Associated with the uplift, large amounts of sediments were eroded and transported down the Green and Colorado Rivers (UGS 2005, Shaagian and Proussevitch 2002). Around 17 Ma, Basin and Range extension began in the area, and produced several small grabens in the quadrangle that mark the transition from the Colorado plateau and the Basin and Range province of the Western United States (Hintze 1988).

Quaternary Period

Erosion has dominated landform development in the quadrangle during the Quaternary Period. Streams in the quadrangle exhibit two terraces above the current stream level, which is incised into the Mancos Shale 3-4 m in some areas.

Chapter 1

Introduction

The Wattis 7.5' Quadrangle is located in the Wasatch Plateau Coal Field (Doelling et al., 1972) in central Utah (Figure 1). The quadrangle contains the Cypress-Plateau coal mine along with the Gordon Creek coal bed methane (CBM) field and Drunkards Wash CBM field, making the quadrangle economically important to the State of Utah.

Few geologic maps including the Wattis Quadrangle are available to the general public. Most of the mapping that has been conducted in this quadrangle has been proprietary work for the Cypress-Plateau coal mine. Available maps include a regional map published by the U.S. Geological Survey (Spieker 1931). Hintze (1993) also published a large regional geological map of the state of Utah. Finally, two 1:100,000 scale geologic map have been published by Witkind et al, (1987, 1995). Tingey (1989) mapped Tertiary dikes, in the region.

Methods

The map was produced by using a combination of aerial photos and digital orthophotoquadrangles. Mapping on aerial photos employed a transfer scope to place contacts on the 1977 edition United States Geological Survey (USGS) topographical base. Mapping on aerial photos was augmented with a Trimble handheld global positioning satellite (GPS) receiver and by triangulation. Strike and dip locations were documented with the Trimble GPS receiver.

The draft map was digitized using Arc View 3.3 and Arc GIS 9.0. Map unit symbols and color codes were selected based on the Utah Geological Survey (UGS) guidelines (Willis and Doelling 1995). Two geological cross-sections were constructed and digitized in Adobe Illustrator CS.

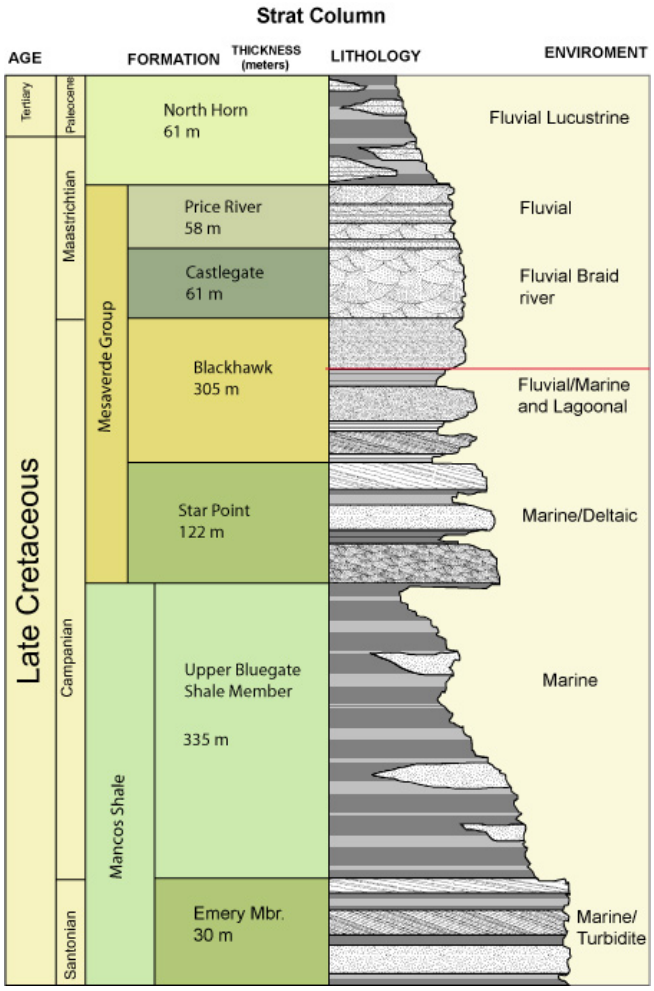

Figure 3. Stratigraphic column for the Wattis Quadrangle. Red line approximates the transition from marine depoits to terrigenous deposits.

Results

Unit Descriptions and Interpretations

The stratigraphy of the quadrangle is descried below, beginning at the base of the exposed section (Figure 3).

Emery Sandstone Member of the Mancos Formation

This unit lies between the well-studied shoreline deposits of the underlying Ferron Sandstone (Turonian) and the overlying Star Point Sandstone (early Campanian; Edwards 2003, Edwards 2001). The Emery Sandstone, which is located in the north central to northeast parts of the quadrangle (Plate 1), is a subangular to subrounded quartz arenite, with minor amounts of feldspar and lithic fragments, with interbedded marine shales (Mattheny and Picard,

1985). Sand grains range from medium to fine, with calcite cement predominating. The sands fine to the north, and 3.5 km to the north of the quadrangle the grains are fine to very fine. The combined sandstone bodies are at least 30 m thick (Figure 4). Individual sandstone beds can be up to 15 m thick. Total thickness also declines east-northeast to just 3 m outside the quadrangle, and pinches out near Price, Utah (Spieker, 1931) 20 km away, consistent with the general sediment transport direction noted by (Edwards, 2003, Edwards, 2001).

Interpretation

The Emery Sandstone comprises three aggradational storm-wave-dominated parasequence sets deposited as waves pushed large amounts of water on the beach and large amounts of sediment were subsequently flushed into the basin, in density or turbidity currents. Evidences for this are Bauma C and D turbidite like units in the sand bodies accompanied by rip-up clasts and scouring of the surface between units of sand. These sands were deposited in relatively shallow water as indicated by the presence of hummocky cross stratification in some sands.

Upper Bluegate Shale Member, Mancos Formation

The Upper Bluegate Shale is located throughout the eastern half of the quadrangle, and is 243-335 m thick from the top of the Emery Sandstone to the base of the Star Point Sandstone. It is a fissile gray to blue-gray rock with interbeds of very fine grained light gray sandstone. Away from the cliffs formed by the overlying Star Point Sandstone, the Upper Bluegate Shale has eroded into low rounded hills that are incised

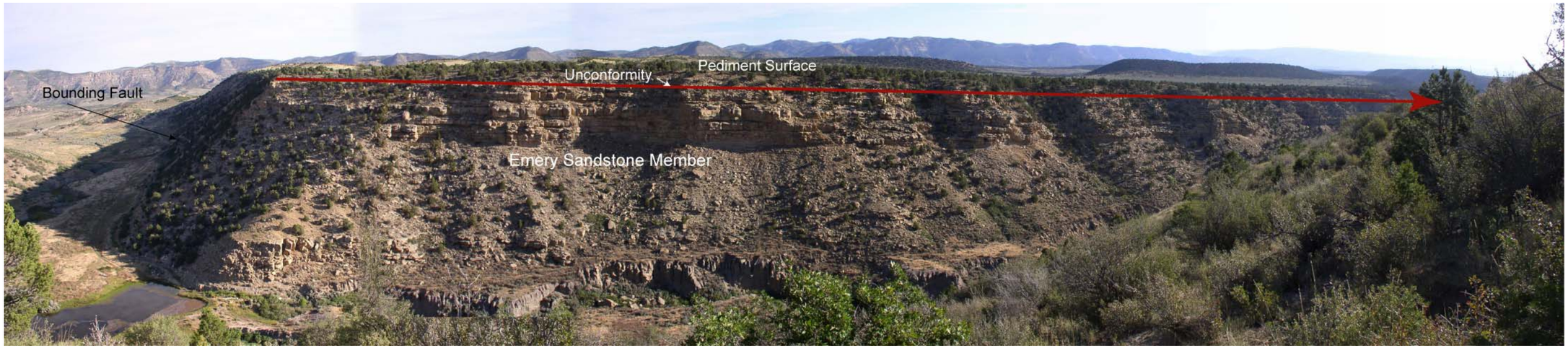

Figure 4. Emery Sandstone with a disconformity between it and Tertiary Pediment debris. The member is 30 m thick, and comprised of three sandstone beds. The lowest bed forms the basal cliffs and is ~ 7 m thick. The middle bed is more easily weathered, and is ~15 m thick. The third sandstone bed is in the upper cliffs and is ~8 m thick.

by intermittent and perennial streams. Where exposed close to cliff faces, the Upper Bluegate Shale forms steep sided hills that resemble badland topography (Figure 5), (Carrol, 1987). The Upper Bluegate Shale is bentonitic, which gives it a popcorn appearance on weathered surfaces (Carrol, 1987).

Interpretation

The Upper Bluegate Shale represents one of the final marine incursions in the Western Cretaceous interior Seaway in Utah (Hintze, 1993). The hills are interpreted to be remnants of former pediments and their cores and have most likely have dictated the location of the present drainages.

Mesa Verde Group

The Mesa Verde Group is a sequence of mainly terrigenous sediments deposited during the final regression of the Cretaceous Interior Seaway, and includes the Star Point Sandstone, Blackhawk Formation, Castlegate Sandstone, and the Price River Formation. These formations are comprised of fluvial sandstone bodies, lagoonal deposits including coal and beach facies, and lacustrine facies.

Star Point Sandstone

The Star Point Sandstone is comprised of three sandstones, which are interfingered with shale bodies (Figure 6). The three sandstones are, the Panther Tongue,

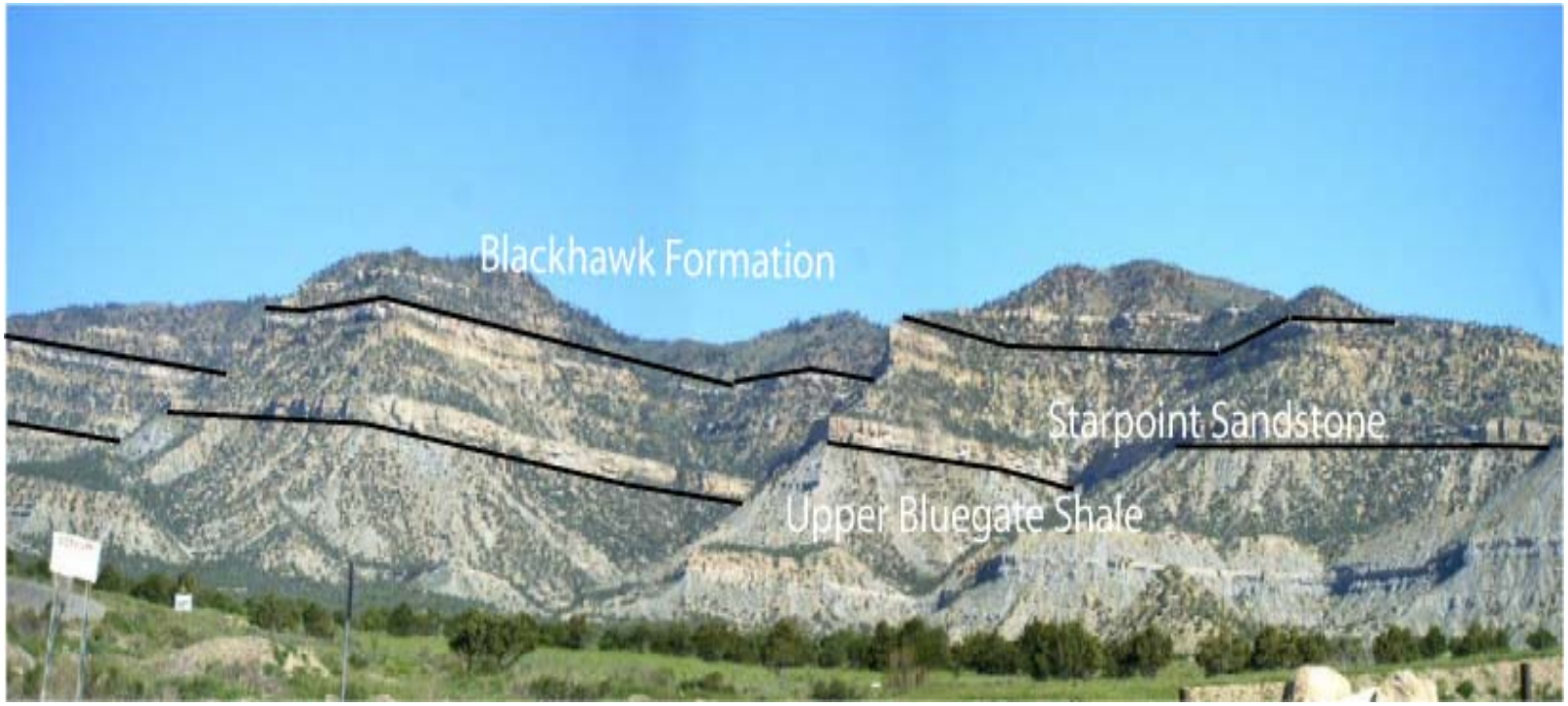

Figure 5. The Blue Gate Member of the Mancos Shale is located at the bottom of the cliffs. The Star Point Sandstone is composed of three sandstone bodies with the lowest one the most prominent in the field area. The Blackhawk formation lies above the Star Point Sandstone and is marked by white foreshore sands, with coal sitting above beach sands.

Figure 6. Interfingering of fluvial-marine sandstones of the Star Point Sandstone with marine shale. The lower sandstone bed in the Panther Tongue Member Member, the middle sandstone bed is the Storres Sandstone, and the top sandstone is the Spring Canyon Member.

Storres, and Spring Canyon Members as designated by Spieker (1931). The total thickness of the Star Point Sandstone in the quadrangle is 122 m.

The Panther Tongue of the Star Point Sandstone is the basal unit and ranges in thickness from 12 to 61 m. In hand sample this sandstone is a tan to beige subrounded quartz arenite with a small amount of feldspar and lithic fragments. *Ophiomorpha*, *Rosella,* and *Skolithos* trace fossils can be found in zones of the Panther Tongue Member, and the top of the unit is marked by an erosional unconformity.

The Storres Member includes a shale unit that separates a sandstone body in the Storres Member from the Panther Tongue Member. The shale is 6 to 12 m thick, and is a blue- gray color. The Storres Member ranges in thickness of 18 m to 24 m, has the same color as the Panther Tongue Member, and contains similar trace fossils (Figure 7). In hand sample, the Storres Member is a subrounded quartz arenite, with minor feldspar grains.

The lower part of the Spring Canyon Member is a shale that lies above of the Storres Member, extending to the base of a coal seam (Spieker 1931). This marine transgressive shale is blue-gray in color and is similar to the shale that separates the

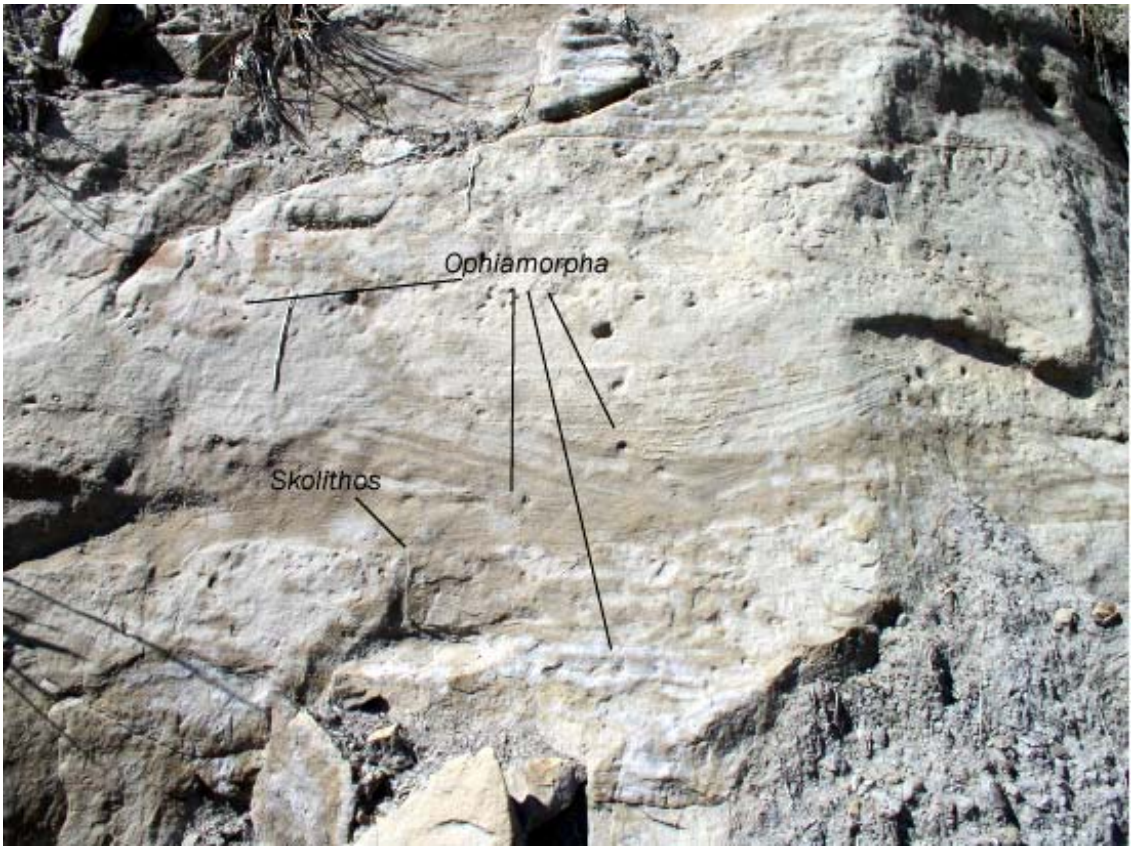

Figure 7. Trace fossils found in the lower shoreface of the middle sand of the Star Point Sandstone. Main traces are *Ophiomorpha,* and *Skolithos*.

Panther Tongue Member and the Storres Member. Above the shale and coal seam, the Spring Canyon Sandstone is a bi-colored quartz arenite: the upper 6 m is white, and the lower 28.3 m is beige to tan in color. The trace fossils are the same as those found in the Panther Tongue Member, and Storres Member sandstones consisting of *Ophiomorpha*, *Rosella,* and *Skolithos*.

Interpretation

The Star Point Sandstone represents lower to upper shoreface sands that prograded during the Campanian eustatic drawdown into the Western Cretaceous Interior Seaway (Elder and Kirkland, 1994).

Blackhawk Formation

Blackhawk Formation lies within the middle of the Mesa Verde Group, and is a major coal-bearing unit (Spieker 1931, 1949), and is located between the top of the Star Point Sandstone and the bottom of the Castlegate Sandstone. The Blackhawk Formation is readily recognized in the area by its white capped sands and its recessive erosional nature when compared to the Star Point and the Castlegate Sandstones (Figure 6). The Blackhawk Formation is 295 to 305 m thick in the Wattis Quadrangle, with thick coal beds (up to 9 m) in the lower portion (Doelling and Smith, 1982, BLM, 2002), although the largest coal seam observed in outcrop is 1.3 m (Figure 8). Thinner coal seams can be found through out the unit. The Blackhawk Formation ranges in color from red-orange, to white, and tan, fine to medium-grained calcite cemented quartz arenite with a sparse weathered feldspars. Shale intercalated in the Blackhawk is composed of three types, including a soft, gray shale, a laminated black to gray carbonaceous shale, and a gray indurated shale found between coal and sandstone (Spieker, 1931).

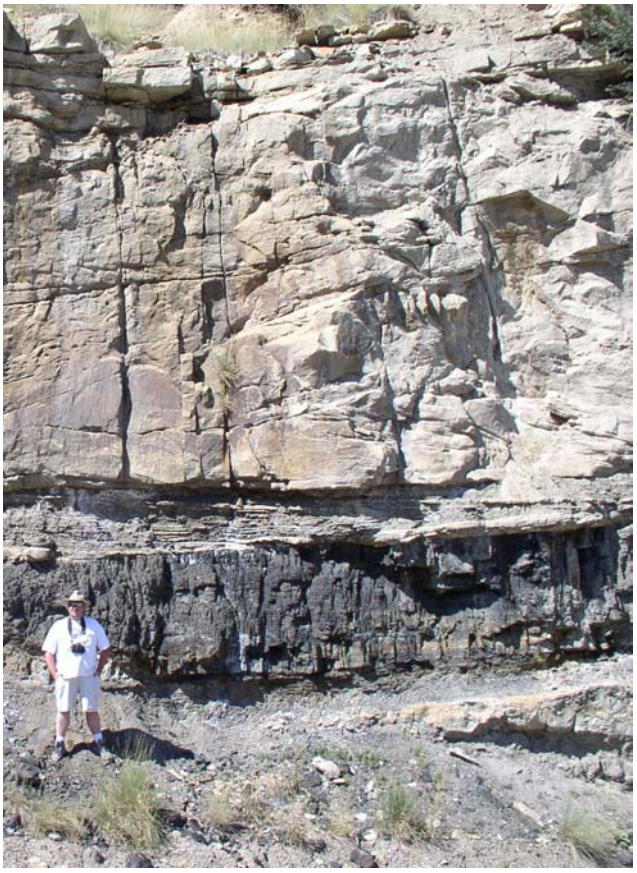

Figure 8. Wattis Coal seam located near the old Cyprus Plateau mine. This seam is 1.2 m thick in this area.

Interpretation

The Blackhawk Formation represents a wave dominated deltaic deposit, with lago0nal and backshore swamp environments. These swamps were dissected by meandering distributary channels represented by the sandstone bodies that erode into the coal seams.

Castlegate Sandstone

The Castlegate Sandstone lies unconformably above the Blackhawk Formation, with the fluvial sands forming the lower half of the higher cliffs in the Wattis Quadrangle. The contact with the Blackhawk Formation is drawn where the uppermost shale of the Blackhawk Formation is in contact with the lowest fluvial sandstone of the Castlegate Sandstone (Figure 9). The Castlegate Sandstone is 61 m thick and appears massive at a distance, but upon closer inspection it is comprised of individual cross-bedded fluvial channel sands. Flow direction in the Castlegate Sandstone was east-northeast (Carrol, 1987). The Castlegate Sandstone is orange to brown in color, and in hand samples, appears to be composed quartz rich sand with some feldspar grains (Carrol, 1987).

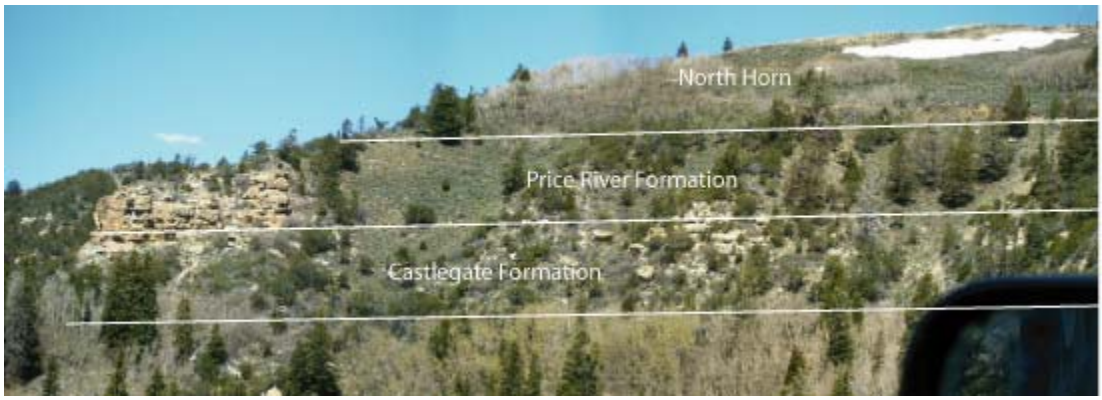

Figure 9. Castlegate Sandstone is found in the lower portion of the cliffs beneath the Price River Formation, which in turn lies beneah the the North Horn Formation that caps the Wasatch Plateau.

Interpretation

The Castlegate Sandstone is a terrestrial deposit representing a fluvial system feeding deltas that lay as far east as the Grand Junction, Colorado area (Demko, 2003).

Price River Formation

The Price River Formation conformably overlies the Castlegate Sandstone (Spieker and Reeside, 1925). The sandstones are mainly coarse to medium-grained with local conglomerates, siltstones, and minor coals (Hansen, 1988). Composition of the detritus is mainly quartz, and quartzite clasts. Thickness in the Wattis Quadrangle is nearly uniform at ~61 m. To the north of the quadrangle, the Price River Formation thickens to as much as 366 m (Spieker 1949).

Interpretation

The Price River Formation is a braided fluvial system, but in most areas preserves more flood plain deposits than the Castlegate Sandstone (Figure 9). Van de Graff (1972) described the Price River Formation as having been deposited by generally west to east flowing coalescing braided and low sinuosity streams that represent the transition between piedmont and fluvial facies.

North Horn Formation

The North Horn formation is reddish brown, and is composed mainly of clay, with a few occurrences of small lenticular fluvial sandstone, marls, and carbaceous shale bodies. The marls crop out only at the highest elevations in the quadrangle, are highly fractured, and are white to yellow-white in color. The thickness is 61 m.

Interpretations

The North Horn Formation unconformably over the Price River Formation (Spieker, 1931, Hansen 1988) and represents a fluvial to lacustrine depositional setting (Figure 9) Maastrichtian to Paleocene in age. The lower portion is fluvial, with a few sandstone bodies deposited by meandering streams, and large flood plain deposits of clay. The upper part of the North Horn Formation is dominated by a lacustrine deposits as indicated by fresh water limestones (Carrol, 1987). The Cretaceous-Tertiary boundary is thought to lie somewhere within the lower part of this formation (Nethercott, 1986, Carrol, 1987, Spieker 1949).

Terrace Gravels and Pediment Structures

Tertiary pediments are found in proximity to cliff fronts and extend outward about 800 m (Figure 10). The pediments were formed by erosion of the Mancos Shale underneath the Star Point Sandstone and Blackhawk formation, causing clasts of the overlying formation to litter the surface of the remnant Mancos Shale, protecting it from continued erosion. These pediments have since become disconnected from the cliffs by erosional dissection. Most pediments are located in the northern half of the quadrangle in the Gordon Creek graben, and are capped with large pebble to boulders sized angular clasts derived from the Star Point Sandstone, Blackhawk Formation, and the Castlegate Sandstone. These pediments dip away from the cliff face at between 10 and 20 degrees, and generally have a slope opposite that of the regional dip of bedrock, creating an angular unconformity.

Figure 10. Pediment surface extending from the base of the cliffs to the valley floor. Pediments are capped by coble to gravel size fragments derived from the Star Point Sandstone, Blackhawk Formation, and Castlegate Sandstone. This cap forms an armor layer protecting from erosion the softer Bluegate Shale Member of the Mancos Formation.

Dikes

Late Oligocene to early Miocene minette and olivine nephelinite dikes in the region were described by Tingey in (1989; Figure 11). Three dikes crop out, with one located in the northeastern corner of the quadrangle, and the other two located at the mouth of Seeley Canyon (plate 1). Width of the dikes varies from 0.4 to 1.2 m, and they can be traced for 10 to 40 m along strike. Most of the dikes have been eroded to the ground surface; however one in Seeley Canyon is about 25 m high. The dikes have been highly altered, and the wall rock has a 0.3 to 0.6 m alteration halo.

Figure 11. Minette dike located at the mouth of Seeley Canyon. These dikes trend roughly east – west. This pinnacle of altered dike and wall rock is ~20 m high.

Figure 12. Modern alluvium comprises the base of this active drainage along with two fluvial terraces. The lower terrace is about 0.33 m above the modern stream, whereas a larger terraces is about 2 m above the current stream bed.

Modern Alluvium

This material is found only in active or recently active stream channels, whether perennial or intermittent. These sediments consist of reworked Mancos Shale, with imbricated sandstone clasts ranging in size from 0.2 to 1.5 m in diameter (Figure 12).

Fluvial Terraces

Two sets of abandoned and elevated (1-2 m) fluvial terraces are most likely Quaternary in age and are

interlayered with local red paleosols. Their composition is dominated by reworked Upper Bluegate Shale and bedding is horizontal.

Structural Geology

The Wattis 7.5' Quadrangle has northeast-southwest trending doubly plunging anticline with 150 m of closure on the surface. The structure is cut by the Gordon Creek graben that is parallel to the structural axis with 30 m of offset (Allis et al., 2002). The basal detachment is in the evaporate section of the Jurassic Arapien Shale (Allis et al., 2002). The northwestern section of the quadrangle has two normal faults that trend northeast to southwest.

CONCLUSIONS

The structure and stratigraphy of the Wattis Quadrangle has been profoundly affected by Basin and Range extension, Laramide and Sevier orogenies, and the Cretaceous interior seaway.

Sediments deposited in the quadrangle rand in age from Santonian (Cretaceous) to the Paleocene in age. The bulk of bedrock was deposited in the Cretaceous Interior Seaway, and is represented by deep marine through costal plain deposits as the Sevier foreland basin was filled by sediments eroding from the Sevier Orogen. These sediments were uplifted during the Laramide orogeny, forming the Gordon Creek anticline. The timing of minette dike emplacement in the quadrangle was between 24 and 8 million years ago (Tingey, 1989). Following dike emplacement, Basin and Range produced the normal faulting in the area, including the Gordon Creek graben, the Cattle Hollow fault, and an unnamed graben encountered in the Cyprus Plateau Coal Mine (personal

communication, David Tingey, 2005). Currently, the Gordon Creek graben, coal bed methane play is a major economic resource in the quadrangle that is producing gas from the Ferron Sandstone Member of the Mancos Formation.

Chapter 2

Introduction

Although others have studied the hydrogeology of the Wasatch plateau, Mayo et al. (2004) recently developed a comprehnsive conceptual model for the groundwater flow within this and other stratified mountainous terranes. They concluded that there are two groundwater regimes, a near-surface active zone where groundwaters becomes progressively older along the flow path, and an inactive zone where the waters all modern. They further concluded these two systems are not in communication with each other. Others have examined the hydrogeology of individual hydrostratigraphic units to determine aquifer conditions such as porosity and permeability, baffles to flow, and flow rates (Gibbs 1998, Bills 2000, Holman 2001, and Black 2000). Modern isotopic data from precipitation events (Zentner, 2001) were compared to isotopic data collected from plateau springs, and was used to develop a model for how precipitation evolves chemically into spring discharge waters.

To understand the hydrogeology of the Wattis 7.5 ‘ Quadrangle, and determine if groundwater can travel from the top of the plateau to discharge at valley margins, groundwater systems were identified using patterns in water chemistry data, local geological setting, and geochemical modeling.

Methods

Water Sampling

Water samples were collected from sixteen springs within the Wattis Quadrangle, and from the Mohrland Mine, located just outside the quadrangle (Figure 13). Water was analyzed for ^{14}C, stable isotopes, solutes and ^{3}H. For the Mohrland Mine, First Water Canyon (FWC) Spring 1, FWC Spring 4, FWC Spring 7, and North Horn Springs 1-4, large volumes of water (15) were needed for ^{14}C analysis due to low bicarbonate concentrations. For all samples water for ^{3}H analysis was collected in 1L brown Nalgene bottles. Stable isotope samples were collected in two 125 ml amber glass bottles with polyseal caps. Water for solute chemistry was collected in 1L plastic bottles and was transported to the lab at ~ 4° C. All bottles were rinsed with distilled water and then precontaminated in the field by rinsing with water from the sample location. Conductivity, temperature, estimated flow rates, and pH were documented at each sample location.

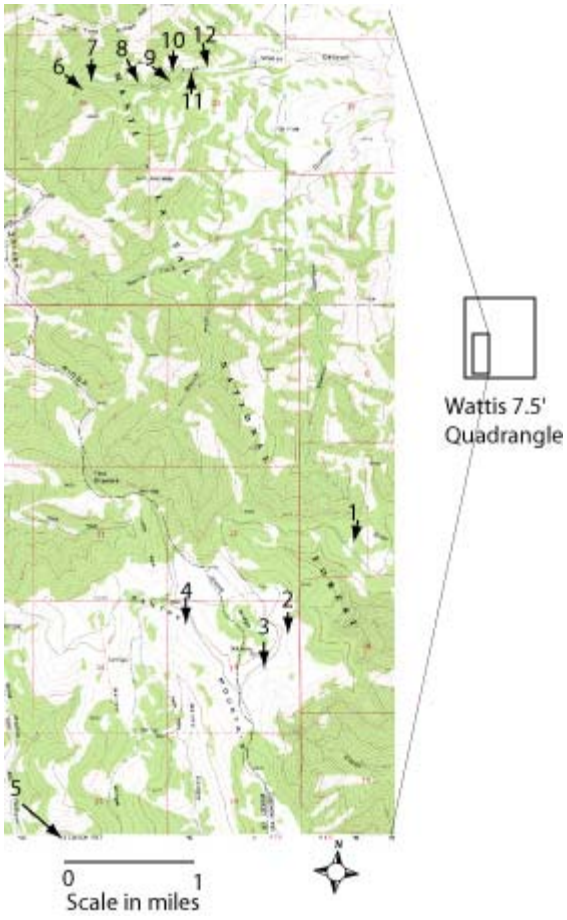

Figure 13. Water sample locations in the Wattis Quadrangle. Samples 1-4 are North Horn Springs, Sample 5 is Mohrland Mine water, and Samples 6-12 are First Water Canyon Springs Below the Blackhawk Formation.

Analytical Methods

Sample analyses for solute chemistry, radioisotopes, and stable isotopes were conducted in the laboratories of the Geology Department at Brigham Young University (BYU).

Cation and Anion concetration

Solute samples were analyzed in accordance with standard EPA methods (EPA, 1983; Pfaff et al., 1991). Bicarbonate concentrations were determined with a Mettler Toledo DL50 Graphix titrator. Anion concentrations were determined with a Dionex 4100 Ion Chromatograph. Cation abundances were measured with a PerkinElmer 5100C Atomic Absorption Spectrometry. The acceptable charge balance error was ≤5%.

Stable isotopes

Stable isotope ratios, δD_{VSMOW}, $\delta^{18}O_{VSMOW,}$ and $\delta^{13}C_{VPDB}$ were measured with a Finnigan Delta^{plus} mass spectrometer equipped with the GasbenchII and HDevice. Methods used for analysis were similar to Epstein and Mayeda (1953), Gehre et al. (1996) and McCrea (1950). δD and $\delta^{18}O$ of lab standards were used to normalize data to the VSMOW/SLAP scale (Coplen, 1998; Nelson, 2000; Nelson and Dettman, 2001) For this study the reproducibility of our internal standard was 0.5‰ (n=13) for δD_{VSMOW} and 0.19‰ $\delta^{18}O_{VSMOW}$ (n=21). $\delta^{13}C_{VPDB}$ values were measured against an NBS-19 calibrated reference gas.

Tritium and ^{14}C

^{3}H and ^{14}C were analyzed at BYU using a PerkinElmer Quantulus 1220 Liquid Scintillation Counter (LSC) for ^{3}H, and Perkin Elmer Guardian 1414 LSC for ^{14}C.

All samples collected were analyzed for ^{3}H, and were prepared for analysis similar to the University of Waterloo Environmental Isotope Laboratory method (Environmental Isotopes Laboratory, 1998), which details the enrichment process. Electrolytic enrichment of potentially low TU waters significantly decreases the lower limit of detection to 0.1 TU (David Tingey, personal communication, 2004).

Analytical standards of a known concentration were mixed for each batch from South Carolina Savannah River Site well P4 water, which has an accepted ^{3}H concentration measured at 0.04 TU, with a NIST tritiated Water. The SC water was also included as an analytical blank in each batch. Samples for ^{3}H were counted in 12, 120 minute cycles, equaling a day of cumulative counting time, for a desired minimum detectable activity (MDA). Final ^{3}H results ± 2 standard deviations in TU were calculated using method of Neary (1997). Reduced data are included in Appendix D.

^{14}C samples were selected on the basis of location, geologic unit at the point of discharge, and possible flow path. Dissolved inorganic carbon was precipitated in the form of $BaCO_3$ as outlined by Clark and Fitz (1997). Benzene synthesis similar to that described by Polach and Stipp (1967) was employed. Benzene was brought to a required counting mass of 2.64 grams (3 ml) with spectragrade benzene and 0.5 ml of scintillation cocktail (POP and POPOP in benzene) was added prior to counting.

Benzene samples were counted in 10, 72 minute cycles, equaling about a half a day of cumulative counting time for a desired MDA. Counting results and statistics were determined by instrument software, and were converted into percent modern carbon (pmc) following Stuvier and Polach (1977). ^{14}C blank made from Uinta Calcite, and a standard made from oxalic acid was used in the counting process for data reduction.

Results

Solute Chemistry

The solute chemistry at each spring and the mine showed little variation during the sampling period; mean compositions are found in Table 1 and Figure 14. The waters from the Wattis Quadrangle are predominantly calcium bicarbonate waters with the exception mine waters of the Blackhawk Formation, which are calcium magnesium bicarbonate waters as shown in Figures 15 and 16. Complete water data are included in Appendix B.

Stable Isotopes

Wattis Quadrangle springs located in the North Horn Formation, Blackhawk Formation, Star Point Sandstone, and Mancos Shale lie close to the global meteoric water line (GMWL) as shown in the Figure 17. The North Horn waters lie slightly above the GMWL, similar to precipitation values of the Wasatch Plateau and many Star Point Sandstone water. Three of the Star Point Sandstone waters lie below the water line along with the mine waters from the Blackhawk Formation.

The North Horn springs have stable isotope values around -16‰ for $\delta^{18}O$ and -121‰ for δD (Table 2). The mines in the Blackhawk Formation have values around -16‰ for $\delta^{18}O$ and -124‰ for δD. The Star Point Sandstone springs have values around -

Table 1. Average solute chemistry for sampled springs and mines in and around the Wattis Quadrangle. All solute chemistry had charge balances ≤ ± 5 %, * represent spring sampling whereas [2] indicate fall sampling events.

	Temp °C	pH	meq														
			TDS	Cations					Anions								
				Ca^{2+}	Mg^{2+}	Na^{+}	K^{+}	Fe^{2+}	HCO_3^{-}	F^{-}	Cl^{-}	NO_3^{-}	Br^{-}	HPO_4^{2-}	SO_4^{2-}	n	stdev
North Horn*	4.5	7.95	8.07	2.77	1.13	0.08	0.04	0.00	3.87	0.00	0.05	0.02	0.00	0.00	0.13	4.00	1.39
Black-hawk[2]	3.1	6.94	23.15	6.29	4.67	0.27	0.12	0.01	7.34	0.01	0.11	0.00	0.00	0.00	4.36	3.00	0.19
North Horn[2]	6.7	7.54	9.58	3.33	1.21	0.09	0.03	0.00	4.72	0.01	0.05	0.02	0.00	0.00	0.14	4.00	1.54
Black-hawk*	4.2	6.94	3.52	1.11	0.29	0.27	0.04	0.04	1.55	0.07	0.06	0.03	0.00	0.00	0.07	3.00	0.30
Upper Star Point	2.3	7.20	3.17	1.10	0.15	0.23	0.02	0.06	1.49	0.02	0.01	0.00	0.00	0.00	0.90	3.00	1.79
Lower Star Point	3.5	7.30	3.58	1.11	0.31	0.28	0.04	0.03	1.56	0.08	0.07	0.04	0.00	0.00	0.06	12.00	1.99
Lindon Rain	-7	5.50	0.30	0.08	0.40	0.30	0.00	0.00	0.08	0.01	0.01	0.00	0.00	0.00	0.02	9.00	0.02

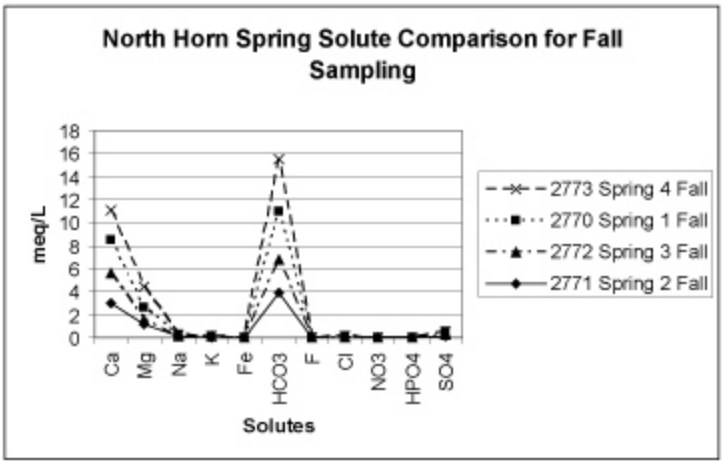

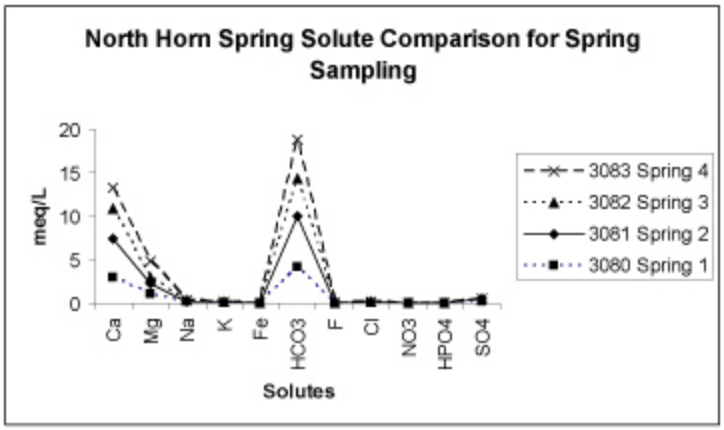

Figure 14. Comparison of North Horn Spring waters for fall sampling events and winter sampling events. Calcium and Bicarbonate are somewhat elevated in spring sampling events when compared to the fall sampling events. However, all samples from the same sample time are similar to each other.

16‰ for $\delta^{18}O$ and -122‰ for δD. The precipitation collected by Zetner (2001) for an area just north of the Wattis Quadrangle has mean values -17.27‰ for $\delta^{18}O$ and -124.38‰ for δD.

The mean $\delta^{13}C$ values for the North Horn springs are -10.23‰ (Table 2), whereas the Blackhawk mines have values of -10.63 ‰, and the Star Point Sandstone springs have values around -10.55‰. Complete isotopic data are located in Appendix B.

Table 2. Mean stable isotopic compositions for the springs. Precipitation data is from Zentner, 2001.

Sample		$\delta^{18}O_{vsmow}$	δD_{vsmow}	$\delta^{13}C_{PDB}$
North Horn Formation	Average	-16.64	-121.21	-10.00
	n	8	8	8
	stdev	0.31	1.91	
Blackhawk Formation	Average	-16.64	-124.01	-10.63
	n	2	2	2
	stdev	0.05	0.01	
Star Point Sandstone	Average	-16.56	-122.47	-10.55
	n	6	6	3
	stdev	0.50	3.56	0.01
Precipitation	Average	-17.27	-124.38	
	n	100	100	
	stdev	3.49	4.50	

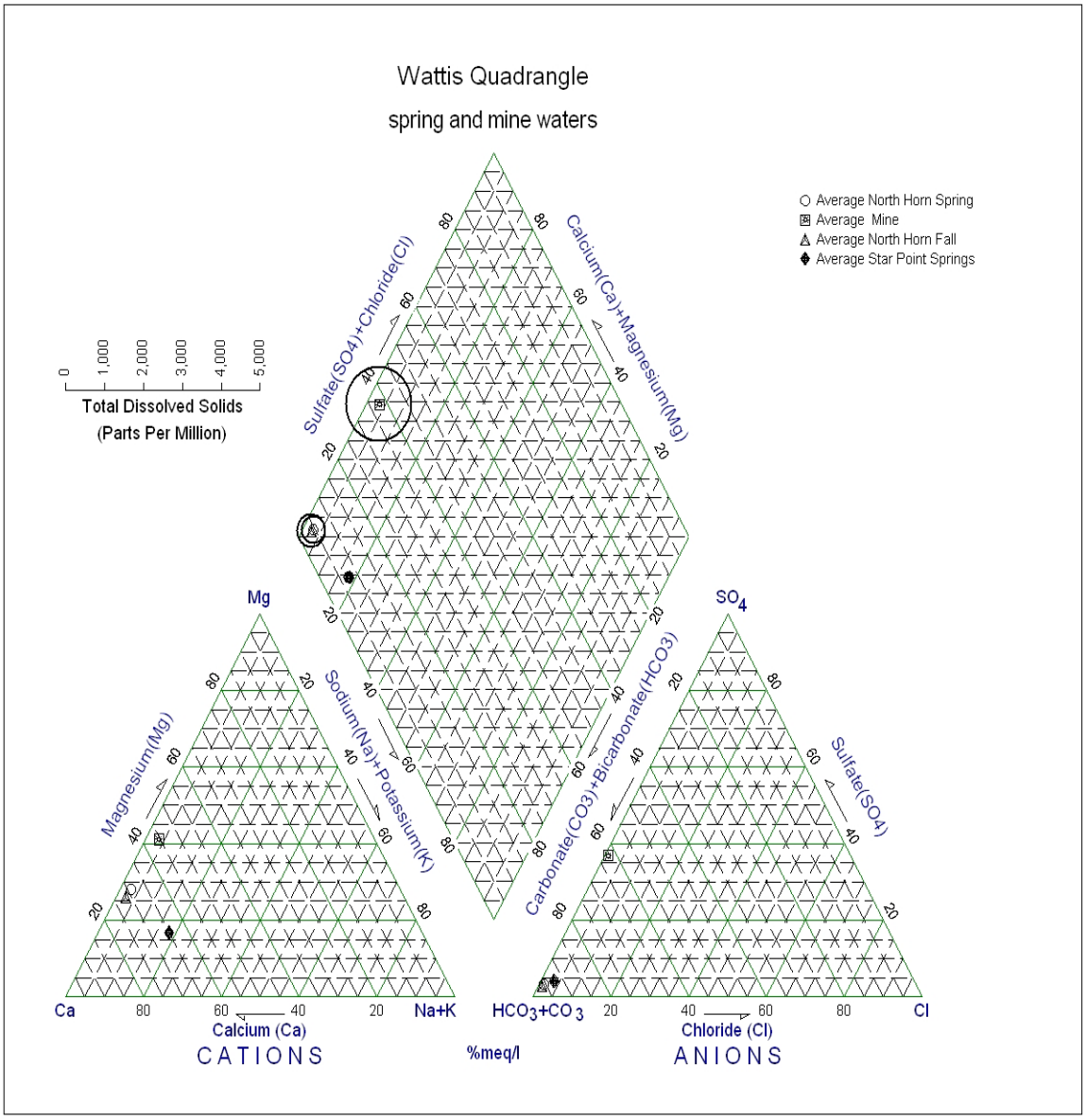

Figure 15. Piper plot of the average spring and mine water compositions. Three distinct groupings of waters exist with the mine waters having the highest TDS, and elevated sulfate. Star Point Sandstone Spring Waters have the lowest TDS.

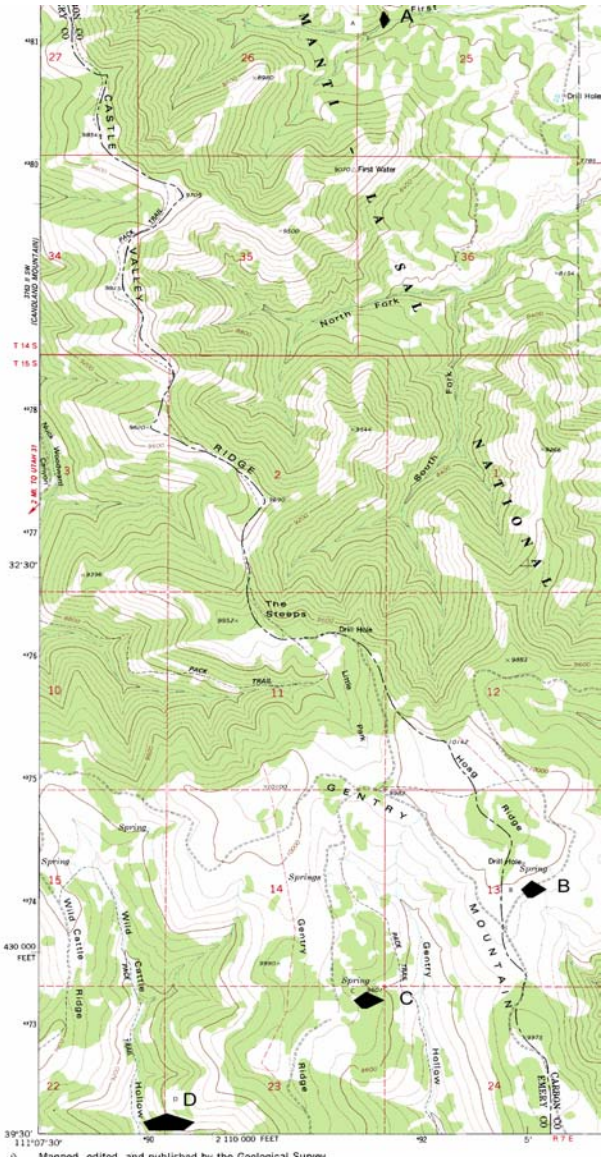

Figure 16. Stiff diagrams of the average solute composition for waters in the Wattis Quadrangle. Most the waters are calcium bicarbonate waters (A, B, C); with the exception of the Morland Mine water (D) that is a calcium-magnesium-bicarbonate-sulfate water.

Radio-Isotopes

^{3}H in North Horn Formation waters during the spring have a mean value of 6.8 TU and in the fall have a mean value of 8.3 TU. Blackhawk mine waters have tritium levels between 2.10 and 4.02 TU. Star Point Sandstone springs have a mean tritium value of 7.50 TU with one outlier of 4.99 TU.

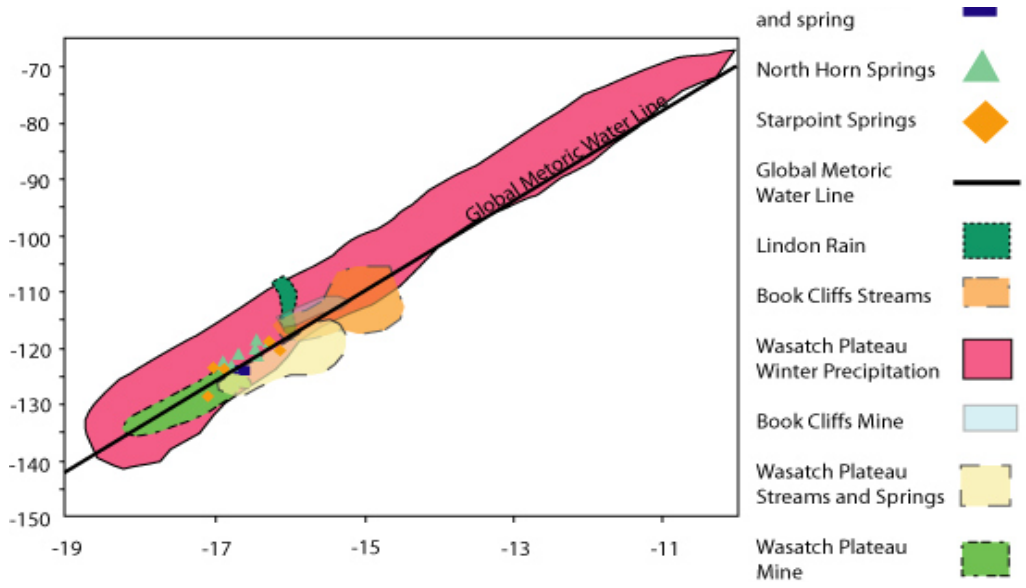

Figure 17. Wattis Quadrangle waters plotted against the global meteoric water line (Fritz, 1997). Wasatch Plateau precipitation data from Zentner, 2001, with Book Cliff data and Wasatch Plateau Springs, Streams, and Mine water data from Mayo et al. (2004) shown for comparison.

The ^{14}C values for the North Horn springs are ~103 pmc, whereas the Blackhawk Mine waters have a value range from 19 to 24.8 pmc. The Star Point Sandstone springs have ^{14}C values ranging from 102.8 to 40.3 pmc. Complete radio-isotopic data are listed in Appendix C.

Discussion

T tests were preformed on data within individual formations to determine if the populations were statistically similar between spring and fall sampling episodes. The α value for the T test was set to .05, and samples that had p values > 0.05 were considered to be different populations, while samples with p values $\leq$ .05 were considered of to be of the same population. T tests were preformed on TDS, and each cation and anion parameter on data located in Appendix D. Samples from North Horn Formation springs for both fall and spring had T test p values of 0.19 or greater for each cation and anion.

Spring and fall samples of the Blackhawk mine waters had $p \geq 0.045$, indicating that seasonal effects on water composition for these two units is not significant.

When comparing Blackhawk Mine waters to North Horn spring waters T tests gave p values of < 0.002, whereas the comparison of Blackhawk Mine waters to Star Point springs gave p values of ~0, demonstrating that these waters are statistically distinct.

NETPATH groundwater modeling was performed to test whether groundwaters in the different aquifers may be related by mixing or chemical evolution. Six possible flow paths were modeled: Lindon Rain to North Horn waters, Lindon Rain to Blackhawk waters, Lindon Rain to Star Point waters, North Horn waters to Blackhawk waters, North Horn waters to Star Point waters, and Blackhawk waters to Star Point waters. Water sampled and analyzed for solutes from Lindon, Utah was chosen as the precipitation endmember it was collected around the same time as the study.

Precipitation was compared to each formation to determine if groundwater discharging from the formations was simply chemically evolved precipitation. Inter-formation modeling enabled the evaluation of chemical evolution along hypothetical flow paths between formations. Ca^{2+}, Na^{+}, Mg^{2+}, Cl^{-}, SO_4^{-}, and ^{13}C were used as constraints, along with the following phases: dolomite, exchange, calcite, pyrite, halite, gypsum, goethite, k-mica, plagioclase AN_{38}, and CO_2 gas. NETPATH found solutions for the evolution of precipitation to waters of the Blackhawk, Star Point, and North Horn Formations (models 1-3, Table 3), whereas no solutions were found for intra-formational flow (models 4-6, Table 4). The results of NETPATH suggest that the water in each unit

is the result of the chemical evolution of recharge water derived from precipitation and that individual aquifers are not in communication.

Table 4. Results of NETPATH models of the geochemical evolution from precipitation to the mean compositions of groundwater in each aquifer.

Initial water	Precip.	Precip.	Precip.
Final water	North Horn	Blackhawk	Star Point
North Horn Springs			
Calcite	0.77		
CO2			
Dolomite	0.55		
Exchange	0.03		
Gypsum	0.06		
K-mica	0.04		
Plagioclase AN38			
Pyrite			
Goethite			
Blackhawk mine			
Calcite		-1.29	
CO2			
Dolomite		2.34	
Exchange		0.12	
Gypsum		2.16	
K-mica		0.12	
Plagioclase AN38			
Pyrite			
Goethite		0.01	
Star Point Springs			
Calcite			0.49
CO2			
Dolomite			0.14
Exchange			0.13
Gypsum			0.02
K-mica			0.04
Plagioclase AN38			
Pyrite			
Goethite			

Note: Results in mmoles/L. Empty cell = no data from formation water or model result did not include the mineral phase. Positive results indicate mineral dissolution or gas consumption. Negative values indicate mineral precipitation or gas production.

Table 3. Results of NETPATH modeling of geochemical evolution of mean composition of North Horn groundwater to mean composition of underlying waters.

Initial water	North Horn	North Horn	Blackhawk
Final water	Blackhawk	Star Point	Star Point
Blackhawk mine			
Calcite	nm		
CO2	nm		
Dolomite	nm		
Exchange	nm		
Gypsum	nm		
K-mica	nm		
Plagioclase AN38	nm		
Pyrite	nm		
Halite	nm		
Goethite	nm		
Star Point Springs			
Calcite		nm	-0.35
CO2		nm	-3.74
Halite		nm	ci
Dolomite		nm	ci
Exchange		nm	0.02
Gypsum		nm	
K-mica		nm	ci
Plagioclase AN38		nm	
Pyrite		nm	-1.07
Goethite		nm	

Note: Results in mmoles/L. ci- models returned only by ignoring one or more constraints-reaction not plausible, nm no models returened; Empty cell = no data from formation water or model result did not include the mineral phase. Positive results indicate mineral dissolution or gas consumption. Negative values indicate mineral precipitation or gas production.

PMC values > 50 % pmc indicate that the water is modern and those samples with values below 50 % pmc have elevated ages based on the following equations.

Equation 1. Soil gas CO_2 has 100 pmc. With the $\delta^{13}C \approx -20$.

$$CO_2 + H_2O \Leftrightarrow H_2CO_3 \Leftrightarrow H^+ + HCO_3^-$$

Equation 2. Mineral dissolution of calcium carbonate from H^+ released in equation 1. $\delta^{13}C \approx 0$, and CO_2 has a pmc value of 0.

$$H^+ + CaCO_3 \Leftrightarrow HCO_3^- + Ca^{2-}$$

Equation 3. The combination of bicarbonate sources from equation 1 and 2 would give a pmc value of 50 pmc at time zero.

$$HCO_{3\,(\text{soil})}^- + HCO_{3\,(\text{mineral})}^- = 50\,pmc$$

Waters from the North Horn Springs all have pmc values around 103, indicating modern water, and no contact with dead calcite. The Blackhawk coal mine waters have pmc values ranging from 19-24.8 with an age range of 7,000 to 9,000 years (Appendix C). The waters collected from the Star Point Sandstone have pmc values between 102 % and 40.3 %, which places these waters between modern and 3,200 years. One water collected from a sandstone bed in the Mancos Shale had a pmc value of 102, which also makes this water modern (Appendix C). Sample 3738 from Appendix A is located at the top of the Star Point Sandstone and has an age of 3,200 years, whereas samples 3737 and 3734, which are all located below the first sample, are all modern waters. This is due to the location of a fault zone below the first spring which allows for rapid infiltration of water along the fault zone and into Star Point Sandstone (Figure 18).

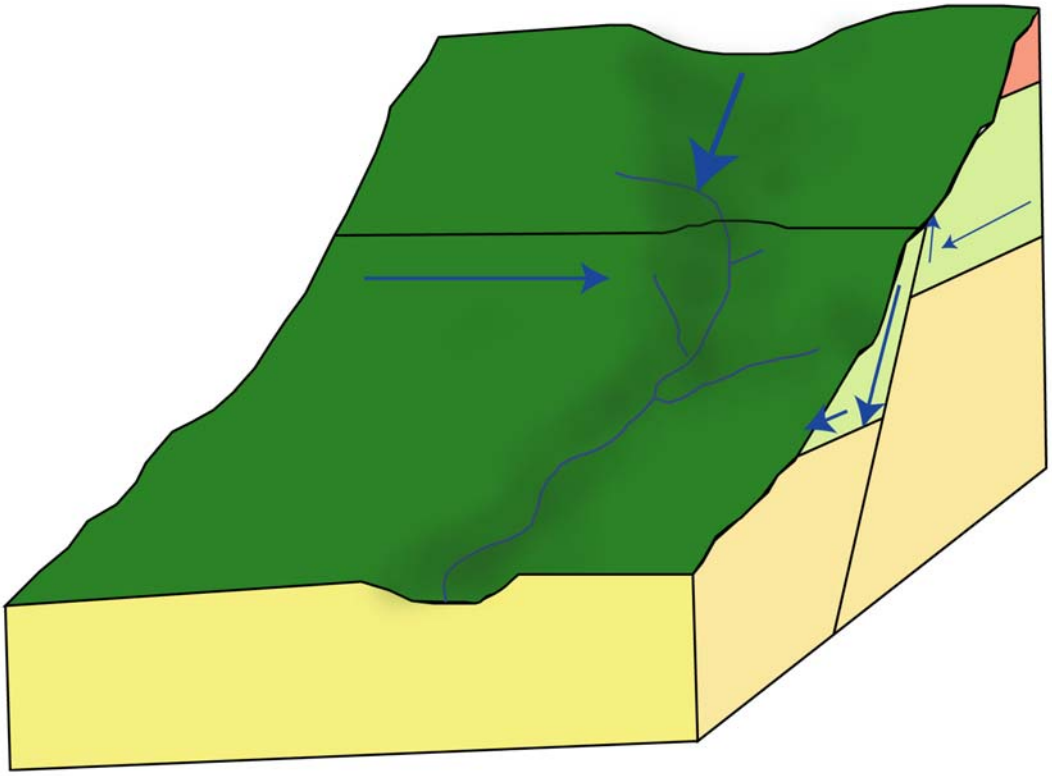

Figure 18. Block diagram showing flow paths for two hydrological systems in the Star Point Sandstone. The fault acts as a conduit for modern precipitation to infiltrate the sandstone bodies. The spring above the fault discharges old water, but exhibits some mixing with modern water due to the local recharge of precipitation. Sandstone bodies below the fault are recharged by precipitation which, then discharges down gradient. Precipitation also flows from the valley walls through the damage zone of the fault, allowing for mixing of old water with modern water.

Current ^{3}H values have returned close to their pre-bomb levels (IEAE, 1998). This value for Utah is around 7 TU. Waters on the top of the plateau have ^{3}H values that range between 11.5 and 5 TU. Waters in the Star Point Sandstone have ^{3}H values between 9.6 and 7.2 TU, only the waters from the Blackhawk formation and the first spring of the Star Point Sandstone have waters with lower ^{3}H values between 4.99 and 2 TU. Samples 2980, 3079, and 3778 (Appendix C) have elevated ^{3}H and ^{14}C ages between 3,200 and 10,000 years ago indicate they are mixed waters. One Star Point spring and the two Blackhawk mines samples probably have tritium in them due to their

close proximity to fault zones (Figure 18) which, allows for mixing of old with modern water. These sampling locations show only minor seasonal variation in discharge, while the other springs in the Star Point and the North Horn Formations have large seasonal variations in discharge, and several of the springs sampled in the North Horn and Star Point were dry during the study due to the extended drought. The water samples from the Wattis Quadrangle fit in the overall trend found by Mayo et al. (2004, Figure 19).

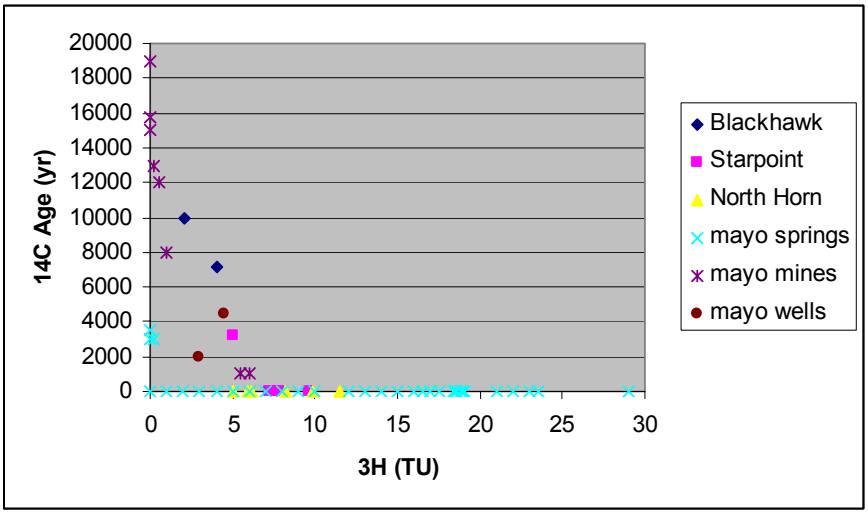

Figure 19. Scatter plot of ^{14}C mean residence times ("age") versus ^{3}H content of surface and groundwater. Data shown are from this study as well as selected data from Mayo et al. (2004).

Conclusions

Groundwaters are divided into three separate systems, which do not appear to mix. North Horn waters on top of the plateau are all modern water that is recharged mainly during winter precipitation events and does not appear to circulate to deeper stratigraphic levels. Storage in aquifers of the North Horn Formation is limited in that during the recent drought most springs dried up. North Horn aquifers are comprised of sandstone bodies that are isolated from surrounding units by shale interbeds.

At a deeper level, mine waters issuing from the Blackhawk Formation and have a ^{14}C age of 7,000 to 9000 years before present, representing early Holocene recharge. Discharge rates do not vary with season. The aquifers of Blackhawk Formation sands drain into the mines. These sands are isolated due to the shale layers from the lagoonal mudstones, and boundaries within the sandstones (Holman, 1999). The Blackhawk mine waters are mixed since they have elevated ^{3}H, which is due to precipitation traveling down the cattle hollow fault zone and mixing with the water in the Blackhawk Formation. In reality the water from the Blackhawk behind the fault is older than 7,000 to 9,000 years before present.

Some groundwater in the Star Point Sandstone is also a mixed system with old water discharging from sandstone bodies that mixes with water flowing along the fault damage zones that cut the valley. Some of the Star Point Sandstone springs, by contrast, discharge modern water that enters the system by recharge in the damage zone of a fault.

Chapter 3

Economic Geology

Coal Deposits

Most of the coal in the Wasatch Plateau field is found in the lower third of the Blackhawk Formation. Eight individual beds containing coal >1.8 m thick have been identified. Major coal bed groups of the Wasatch Plateau include, in ascending order, the Hiawatha zone (consisting of the Knight, Accord Lakes, Axel Anderson, and Cottonwood beds), the Blind Canyon zone, the Wattis zone, the Gordon zone, the Castlegate A zone, and the Castlegate D zone (BLM 2002, BLM 2002, Gloyn, 2003). The thickness range of minable coal for north central part of the Wasatch Plateau field is shown in Table 5.

Table 5 Range of coal thicknesses for the central Wasatch Plateau coal field. The coal seams thicken further to the west under the plateau. Chart modified from BLM (2002; Appendix 25).

North Central Wasatch Plateau beds	Thickness Range (m)		
Gordon zone (Bob Wright-Mckinnon)	1.8	to	5.5
Wattis	1.8	to	4.9
Cottonwood (Hiawatha)	1.8	to	8.8
Axel Anderson (Hiawatha)	1.8	to	4.6
Acord Lakes (Hiawatha)	1.8	to	4.6
Blind Canyon	2.2	to	7.7
Knight	1.8	to	5.2

The coal beds have a gentle slope of 2° to the west in the Wattis Quadrangle and are cut by north south trending normal faults that locally drop the coal out of mining area. However, the grabens are generally small enough that the mines can cut through the sandstone bodies and continue mining on the other side. (Doeling, 1972, David Tingey, personal communication 2005).

Coal mining in the Wattis Quadrangle began in 1916 and continued until 2001. Mining began in Service Bay Canyon in the Wattis Seam, by the Wattis Coal company, which was subsequently merged with Lion Coal company in 1919 (Strack 2001). Lion Coal Corporation operated the Wattis mine until 1964. Mountain States Machinery of Salt Lake City purchased the mine for its salvage value. In 1967 the Wattis property, consisting of the Wattis Seam (3 meters average thickness), the Third Seam (3 meters), and the Hiawatha Seam (2 meters), was sold to Plateau Mining Company. Plateau Mining Company was sold to Cypress Coal Company, which operated the mine until it closed in 2001 (Strack 2001).

Coal quality

The coals of the North Central Wastach Plateau field are usually of good quality, having low ash and low sulfur contents, with high Btu/lb yields. Most the coals are high-volatile C bituminous coal, with some coals in the high-volatile B bituminous coal range (BLM 2002, and Gloyn et al., 2003). These coals may have relatively high resin content between 2 and 15% by volume (Tabet et al., 1995a). Coal quality statistics are summarized in Tables 6 and 7 for the Blind Canyon coal seam and the Hiawatha coal zone.

These two coal zones have similar coal quality content with high heat content, and low ash and sulfur content. It has been reported that coals further to the south have a higher ash and lower heat content (BLM, 2002, and Gloyn et al., 2003).

Table 6 Coal quality statistics for the Blind Canyon bed of the Blackhawk Formation, Wasatch Plateau coal field (BLM, 2002; Gloyn et al., 2003).

	Mean	Maximum	Minimum	Standard Deviation	Sample Population
Ash %	7.1	18.3	2.3	2.3	144
Btu/lb	12,844	13,966	10,800	463	142
Fix. Carbon (%)	44.96	50.08	37.5	2.12	136
Vol. Matter (%)	42.8	48.4	0.29	1.7	139
Sulfur (%)	0.52	1.1	1.2	0.14	130
Moisture (%)	5.13	8.37	1.11	1.11	145
Carbon (%)	72.74	80.5	3.15	3.15	21
Hydrogen (%)	5.72	6.66	0.48	0.48	21
Nitrogen (%)	1.3	1.6	0.2	0.2	20
Oxygen (%)	11.81	16.5	1.94	1.94	21
Chlorine (%)	0.01	0.03	0.01	0.01	8

Coal Resources

The Wasatch Plateau is a major Utah coal field with resources in excess of 10.2 billion tons of coal (Doelling, 1972); however, the BLM Price Field office estimates a resource base of 1.05 billion tons of in-place coal based on the following criteria: coal beds generally greater than 2.2 m thick, and with at least 61, but less than 769 m of overburden. The coal resource estimates reported here were recalculated for this study to conform with mining and recovery parameters that the BLM felt would allow the coal to be economic to mine in the next 30 years (BLM, 2003).

Table 7 Coal quality statistics for the Hiawatha bed of the Blackhawk Formation, Wasatch Plateau coal field (BLM 2002; Gloyn et. al. 2003).

	Mean	Maximum	Minimum	Standard Deviation	Sample Population
Ash %	6.67	25.72	0.05	1.98	521
Btu/lb	12,689	14,530	9,073	487	521
Fix. Carbon (%)	45.64	54.4	31.26	1.89	502
Vol. Matter (%)	42	47.4	4.4	2.3	509
Sulfur (%)	0.63	4.06	0.29	0.25	479
Moisture (%)	5.55	14.24	0.7	1.58	537
Carbon (%)	71.6	81.88	51.38	6.05	58
Hydrogen (%)	5.51	6.3	3.89	0.51	58
Nitrogen (%)	1.3	1.7	0.3	0.2	58
Oxygen (%)	12.18	17.18	9.25	2.18	58
Chlorine (%)	0.05	0.13	0	0.04	22

A little over 330 million tons of coal has been defined as likely to be mined between 2003 and 2017, with a little over 720 million tons of coal available for mining from 2018 through 2032. Of the coal that is likely to be mined in the next fifteen years, over 94% is found in the Hiawatha and Wattis zones (BLM, 2002). Only about 20 million tons of the mineable 1.05 billion tons of coal or 1.9% falls into the 2-2.3 m thick category, the rest is thicker, summarized in Table 8.

Table 8 Remaining, known and estimated in-place coal resources by mining period for the Wasatch Plateau coalfield within Carbon and Emery Counties, including the Wattis Quadrangle, given in million of short tons for coal beds mostly > 1.8 m thick, and with > 61 m, but < 769 m of overburden, data from BLM (2002).

Mining Period	Demonstrated (tons)	Inferred (tons)	Total (tons)
2003-2017	308.1	23.6	331.7
2018-2032	688	35.1	723.1
Total	996.1	58.7	1054.8

Coal bed Methane

Most the coal bed methane (CBM) comes from coals located within the Ferron Sandstone Member of the Mancos Formation. The Ferron coals were deposited in the Vernal delta, which can be traced from Price, Utah as far south of the town Orangeville, Utah (Gloyn et al., 2003). There are two areas of thin coals in the northern part of the Ferron coal bed trend (Tripp 1998) shown in Figure 20. The thicker coal deposits in this area comprise three to six beds, and can total up to 14.6 m thick and average 7 m thick (Burns and Lamarre, 1997, Gloyn et al., 2003).

Burns and Lamarre noted (1997) that coals in the northern Vernal delta have a gas content from 6.25 cm^3/g to 15.66 cm^3/g of coal. Gloyn (2003) reports that these coals of the Vernal delta have high gas content and can be commercially developed. To date, most of the production from the Wattis Quadrangle has come from the Drunkards Wash play,

which has produced over 232,000,000 million cubic feet (Mcf) of gas and over 91 billion barrels (bbl) of water from 360 wells in Carbon County (Table 9; Gloyn et al., 2003).

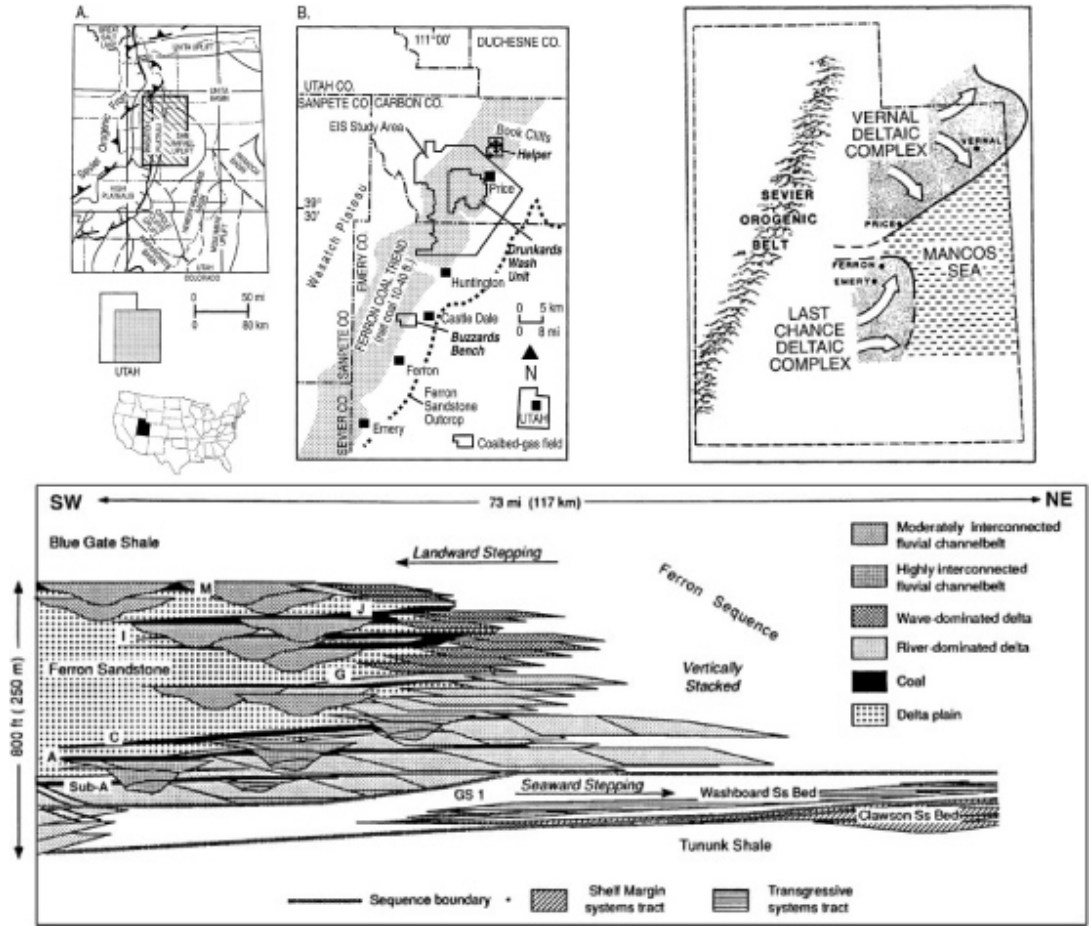

Figure 20. A and B show the location of the Ferron Coal trend in Emery and Carbon Counties. C shows the depositional locations of the deltas that fed the Ferron sands. Figure D shows the depositional environments in the Dunkards wash and Gordon Creek CBM plays. Coals M, J, and I are being produced in the Gordon Creek CBM play. Modified from Montgomery et al. (2001)

Future production in this area could include the possibility of more wells in the Gordon Creek and Drunkards Wash plays, as well as possible production from Emery coals, which do not outcrop in the area, but are known from drilling on the Wasatch plateau (Gloyn et al, 2003). These coals are known to be 6 m thick and at a depth of 610 to 1524 m, which Gloyn et al. (2003) concluded are at a reasonable depth for gas production. However, no data have been released on the gas content of these coals.

Table 9. Total production data for the Drunkards Wash CBM gas field as of June 30, 2001. Since these data were reported, the Gordon Creek CBM play has been added to the Carbon County production in the Wattis Quadrangle. There also has been a significant increase in the number of well that have been drilled in the past few years. In 2003 around 600 new wells were drilled in the Drunkards Wash play. Table modified from Gloyn (2003).

Carbon County					
Field	Discovery Date	Oil	Gas (Mcf)	Water (bbl)	Number of Active Wells
Drunkards Wash	1991	0	232,669,588	91,102,364	304
Emery County					
Field	Discovery Date	Oil	Gas (Mcf)	Water (bbl)	Number of Active Wells
Drunkards Wash	1991	0	4,336,485	3,528,554	57

CO_2 gas

Wells of the Gordon Creek field, discovered in 1947, penetrate the Permian Kaibab Formation (Black Box Dolomite Member), the White Rim Sandstone of the Cutler Group, and the Sinbad Limestone Member of the Moenkopi Formation, and have shown CO_2 gas. Gordon Creek wells reports 99 % CO_2 purity (Gloyn et al., 2003). The Kaibab Formation is 30-38 m thick and consists of silty, cherty, dolomitic limestone, and represents an epicontinetal marine transgression. The average pay thickness is estimated to be 10 m (Gloyn et al., 2003). The White Rim Sandstone Formation represents a costal dune deposit that is 120-200 m thick in this area (Gloyn et al., 2003). The following Table 10 shows data from the Gordon Creek field. The first well that was drilled in the Gordon Creek field had gas flow at an estimated rate of 8,900 Mcf/day from the Permian White Rim Sandstone and 8,500 Mcf/day from the Sinbad Limestone Member of the Triassic Moenkopi Formation (Allis et al., 2002).

Table 10. Reservoirs of non hydrocarbon gasses in the Gordon Creek Field (from Allis et al., 2002)

Gordon Creek								
White Rim Sandstone Reservoir								
Area of Reservoir (km^2)	Average Depth (m)	Lithology	Net Thickness (m)	Net Pay (m)	Lithology of Seal	Gas Composition	Production History	Porisoity Premeability (%)
34	3900	Sandstone	150-200	50	dolomite	98.82% CO_2, 1.03% N_2	None	8 to 12 intergranular and fracture
Moenkopi Formation, Sinbad Limestone Member								
Area of Reservoir (km^2)	Average Depth (m)	Lithology	Net Thickness (m)	Net Pay (m)	Lithology of Seal	Gas Composition	Production History	Porisoity Premeability (%)
34	3340	limestone	15-18	7 m	shale and siltstone	99.5 % CO_2	none	6 fracture
Kiabab Formation (Black Box Dolomite)								
Area of Reservoir (km^2)	Average Depth (m)	Lithology	Net Thickness (m)	Net Pay (m)	Lithology of Seal	Gas Composition	Production History	Porisoity Premeability (%)
34	3868	dolomite	30-38	10	unconformity	99 % CO2	None	6 to 8 Fracture

High flow rates suggest the presence of fractures in the producing formations. The structure of the field is a northeast--southwest trending doubly plunging anticline with 150 m of closure on the surface. The structure is cut by the Gordon Creek graben that is parallel to the structural axis with 30 m of offset (Allis et al., 2002). The basal detachment is in the evaporate section of the Jurassic Arapien Shale (Allis et al., 2002). Estimated potential recovery of CO_2 from the White Rim Sandstone and the Sinbad Limestone is 140 billion cubic feet of Gas (Bcf) (Allis et al., 2002).

Other Deposits

The Wattis Quadrangle does not have any known deposits of precious or base metal ores, but it does contain material that could be suitable for buildings and landscaping. The Star Point Sandstone, Emery Sandstone, and the Castlegate Sandstone all could be used for flagstone paving, building veneer, etc. Due to the highly fractured nature of these sandstone bodies, their use as building stone would be limited. The area

also has a large quantity of possible lightweight aggregate in the form of bloated shale, including the Upper Bluegate Shale Van Sant (1964). The Sandstone bodies may also be used as crushed roadbed aggregate in the construction roads. Large pediments of gravels from the Star Point Sandstone, Blackhawk Formation, and Castlegate Sandstones could be used for paving and road base as well (Hansen, 1988). These resources have not been developed, however.

Conclusions

The Wattis 7.5 Minute quadrangle has several viable energy resources for the State of Utah. With the quadrangle being located in the Wasatch Plateau coal field, and includes the Gordon Creek and Dunkards Wash plays for coal bed methane. Along with these energy sources, large amounts of CO_2 are stored in deeper formations. This resource could be used for enhance oil recovery in the near by oil fields of the Uinta Basin, for example. The quadrangle also has large amounts of aggregate and stone that could be mined and used for build material, or decorative work, but these resources have not been exploited as of yet.

Chapter 4

Sequence Stratigraphy

Introduction

Sequence stratigraphy as a concept was developed in the late 1970's (Boggs 1995, van Wagoner 1995, and Mitchum et al 1977). The Blackhawk Formation in the Book Cliffs of central Utah, around the Price-Helper area, have been studied by the major oil companies as an analog for modern parasequences and sequences (Van Wagoner et al. 1990, Van Wagoner et al. 1995, Holman 2001). Recently, other formations of the western Cretaceous Interior Seaway have been studied for sequence stratigraphy, namely the Ferron Sandstone Member of the Mancos Shale, Castlegate Sandstone and Star Point Sandstone (Holman 2001, Dewey, 1997).

The Emery Sandstone of the Mancos Shale has been interpreted to be a fluvial-marine transitional sandstone body that prograded into the Western Cretaceous Interior Seaway (Matheny and Picard 1985, Edwards et al. 2003). Edwards (2003) identified 17 parasequences arranged into three 600 kyr regressive-transgressive cycles. The Emery Sandstone was deposited at a storm-dominated shoreline (Edward et al. 2003, Edwards et al. 2005). The general sediment transport was from the south south-west to the north north-east direction with the sediments fining further north (Matheny and Picard 1985, Edwards, 2003).

The Star Point Sandstone is composed mainly of fluvial deltaic sediment (Demko, 2003), and is located in the western part of the quadrangle and comprises the lowest cliff-forming unit. The general transport direction was initially to the southwest and changing later to the northeast (Edwards et al. 2001). Eight to nine parasequences are arranged into three transgressive-regressive cycles.

Local study of the sequence stratigraphy in the Lower Mesa Verde Group, in partiuclar the Star Point Sandstone and Emery Sandstone Members of the Mancos Shale was conducted to identify the number of parasequences and sequences in these sandstone bodies, and to identify the depositional environment in the context of regional patterns.

Methods

Emery Sandstone

Emery Sandstone sections were measured in six locations (Figure 21), and were examined for sedimentary structures, erosional surfaces, boundaries, degree and type of bioturbation, sediment thickness, and texture. Detailed drawings of the outcrops were made, and depositional conditions were inferred from the sedimentary characteristics. Correlations between the locations were made similar to the method described by Taylor and Lovell (1995).

Star Point Sandstone

Star Point Sandstone outcrops were examined in three major canyons in the Wattis Quadrangle shown in Figure 21. These outcrops were measured, and detailed descriptions were made of the sedimentary structures, bioturbation, texture, and thicknesses. Drawings were created from the field notes and correlation between the three locations was made, allowing for the interpretation of depositional setting for this unit.

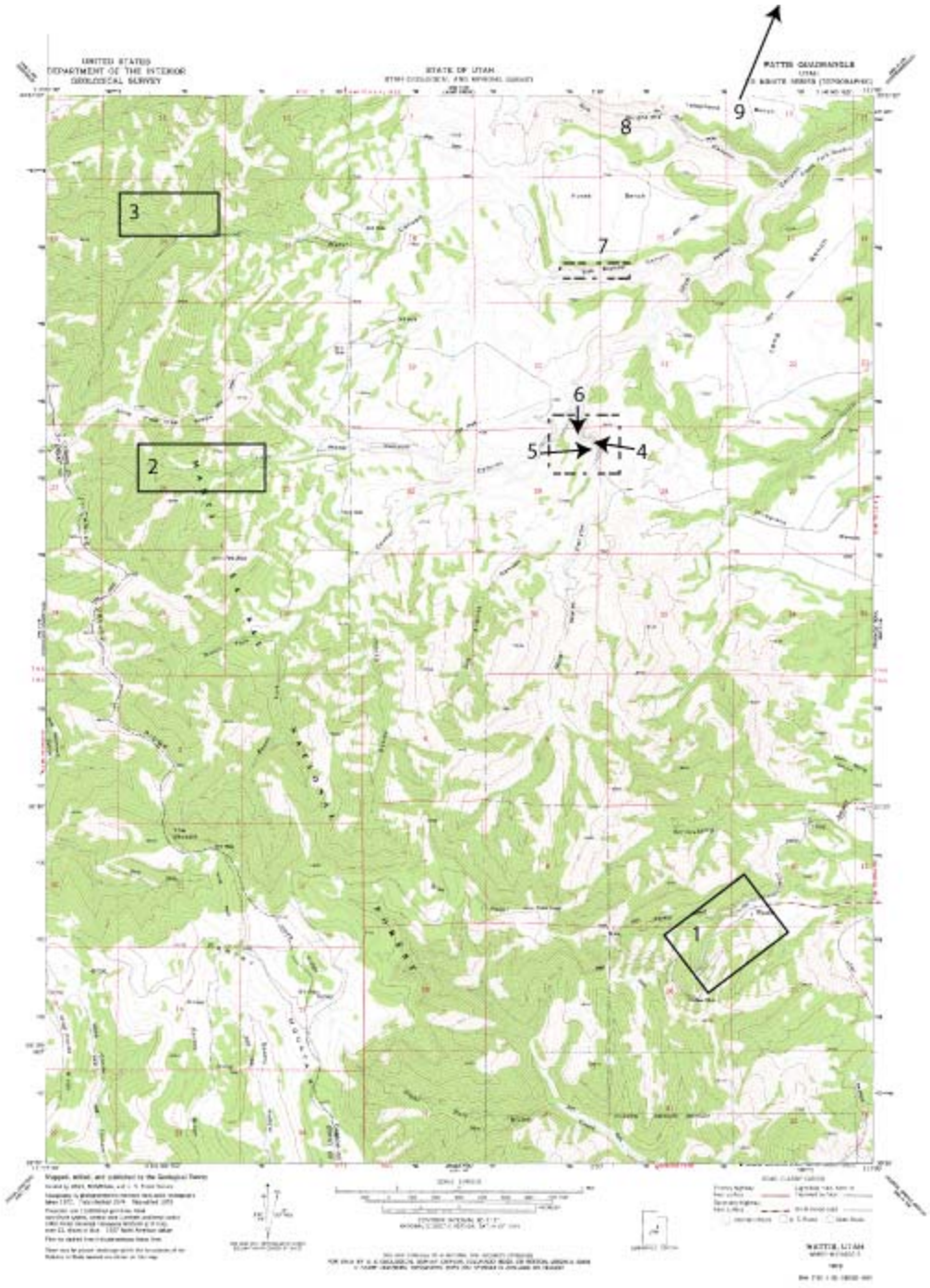

Figure 21. Location of the Star Point Sandstone and Emery Sandstone parasequences described in this study. Solid boxes and numbers 1- 3 are locations of the Star Point Sandstone parasequences. Dashed boxes and numbers 4 – 9 are the parasequences of the Emery Sandstone.

Results

Emery Sandstone

Data collected at six locations, shown in Figure 21, are summarized in Table 11. These outcrop locations were chosen because of access and exposure, with most outcrops having good exposure along strike and dip, providing the opportunity to examine the outcrop in three dimensions.

Table 11. Sequency stratigraphy data for the Emery Sandstone of the Mancos Formation, and the Star Point Sandstone. Ophi=*Ophiomorpha*, and Rosse=*Rossella, DLS= Distal Lower Shoreface, PLS = Proximal Lower Shoreface, USF = Upper Shoreface*.

Emery Sandstone						
Location	**1**	**2**	**3**	**4**	**5**	**6**
# of parasequnces	2		3	4	4	1
Thickness of parasequence sets	~10 m	.2-.7m	3-15 m	4-20 m	2-20 m	1.5m
Depositional enviroment	DLS-PLS	DLS	DLS-PLS	DLS-PLS	DLS-PLS	DLS
Trace Fossils	*Ophi*	*None*	*Ophi & Rosse*	*Ophi*	*Ophi & ?*	*None*

Star Point Sandstone			
Location	1	2	3
# of parasequnces	3	3	3
Thickness of parasequence sets	30-50 m	20-55m	30-50m
Depositional enviroment	DLS-USF	DLS-USF	DLS-USF
Trace Fossils	*Ophi & Skolithos*	*Ophi, Rosse, Skolithos*	*Ophi, Skolithos*

Main trace fossils found in the Emery Sandstone are *Rossella*, and *Ophiomorpha*. *Ophiomorpha* is found in all but two of the six sections, whereas *Rossella* is found at only one. These trace fossils indicate normal marine environment located in the lower shoreface of the Emery Sandstone. These trace fossils are located mainly in sandy units, with the smaller sandstone lenses being highly bioturbated, and the large sandstone lenses having biotrubation limited to the upper meter.

At the six study locations the Emery Sandstone is a package of alternating sandstones and shale. Shale units represent the base of parasequences (deeper water), whereas the sandstones represent upward shallowing marine environments. Bedding in

the sandstone bodies ranges from hummocky cross stratification to laminar and trough cross stratification, with some dish and pillow structures.

Star Point Sandstone

Three main sand bodies make up the Star Point Sandstone, and are separated by two shale layers (Table 11). The lowest sand body is the Panther Tongue that has an upper erosional surface that is marked with rhizoids and small dissolution cavities. There are several beds of hummocky cross stratification indicating lower shoreface conditions, with laminar beds, which are bioturbated by *Skolithos,* and *Ophiomorpha*. Upward through the section, these laminar beds transition into trough cross stratification. This pattern is repeated three times until blue-gray marine shale is deposited on top of the erosional surface.

The middle sand package is thinner at locations one and three compared to location two. Major Sedimentary features in the second sand are hummocky cross stratification, with some laminar bedding, as well as *Skolithos* and *Ophiomorpha*.

The upper-most sand package has five deepening and shallowing events with the last one showing foreshore sands. On top of the foreshore sands is the first coal seam of the Blackhawk Formation. Major sedimentary feature include hummocky cross stratification, laminar beds, and trough cross stratification. The foreshore sands on the last parasequence are white, whereas the other sands are tan. The foreshore sands are well sorted and well rounded.

Discussion

Emery Sandstone

The Emery Sandstone comprises three sand bodies in the quadrangle shown in Figure 22. At the base of the first large sandstone layer are several small sand lenses with hummocky cross stratification (HCS) that are interpreted to be formed by scouring of the ocean bed by storms waves below fair-weather wave base but above storm wave base (Prothero, 1990) . Soft sediment deformation suggests major storms suspended large amounts of sediment in the water column and allowed for water to be trapped in the sediment. Subsequent burial and dewatering produced dish and pillow fluid escape structures (Figure 23), typical of the distal lower shoreface (Van Wagoner et al. 1990).

Figure 22. Three parasequences located in the Emery Sandstone. Parasequence A is the 7m thick, B is 3 m thick and C is 4 m thick in this area.

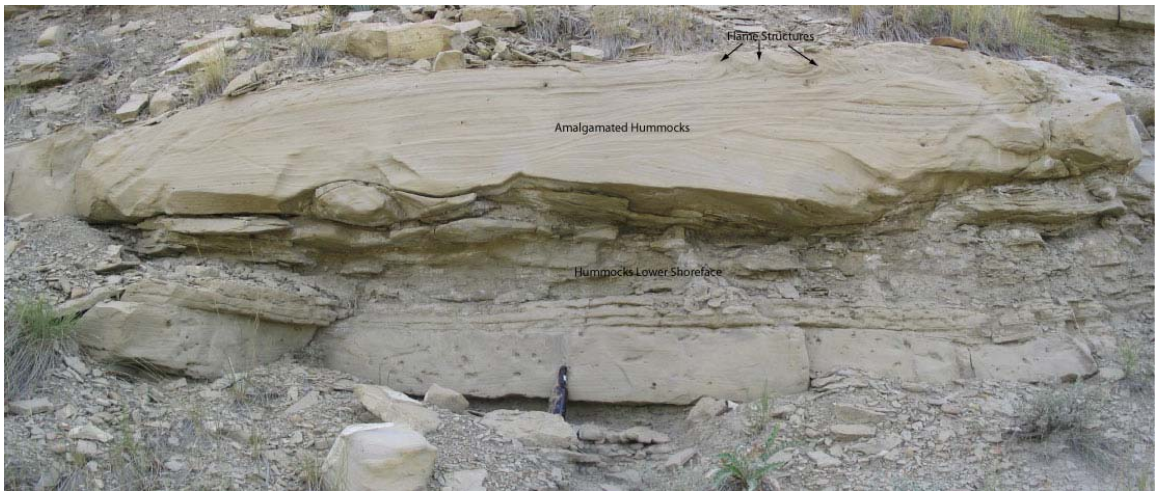

Figure 23. The lower sand of the Emery Sandstone contains normal amalgamated hummocks that have been extensively bioturbated by *Ophiomorpha,* and *Skolithos*. The middle mud contains some hummocks from the distal lower shoreface. The upper sand contains more amalgamated hummocks that have little bioturbation, but have dish and pillow fluid escape structures at the top.

The large sand packages have amalgamated hummocks at the bottom and then transition upward into laminar beds, and finally cross beds near the top. Subsequently, a deepening of the marine environment allowed for the development of amalgamated HCS, (Figure 24). The large sand packages transition laterally to the west into small packages of amalgamated hummocks (Figure 25). These large sandstone bodies have been interpreted as possible storm relaxation channel sands that grade laterally into overbank deposits. The large sands packages also thin to the north, and at the sample location one, (Figure 21) only the uppermost sand of the Emery is present as a 1 m thick bed of amalgamated HCS (Figure 26). The following schematics show the Emery Sandstone from the west to east and from south to north (Figure 27). Based on the sedimentary features found in the sand packages, it appears that large storms pushed large amounts of sand to the beaches and further inland, followed by a backwash of water that was loaded with sediment, creating a density current that redistributed the sand seaward in channels of turbidite-like material. These density currents deposited the laminar sand and cross

bedded sands of the lower shoreface, and repeatedly punctuated normal marine sedimentation. This type of deposition is similar to deposition along the Atlantic coast following major storms.

Figure 24. Large photo shows the complete upper parasequence of the Emery Sandstone. Inset A shows the distal lower shoreface composed of mudstones with hummocky stratification. Inset B shows the proximal lower shoreface consisting of amalgamated hummocks. Inset C shows the laminar beds representing Bauma C and D beds. Inset D shows unidirectional cross bedding near the top of the parasequence.

Figure 25. Emery Sandstone adjacent to the thick sandstone outcrops shown in Figure 23. Only thin sandstone bodies are present and consist of hummocky cross stratification covered by mudstone, representing sand deposited in the distal lower shoreface.

Figure 26. Top sandstone body of the Emery Sandstone located ~ 12 km north of the Wattis Quadrangle showing dramatic thinning. Sand bodies contain t hummocky cross stratified sands.

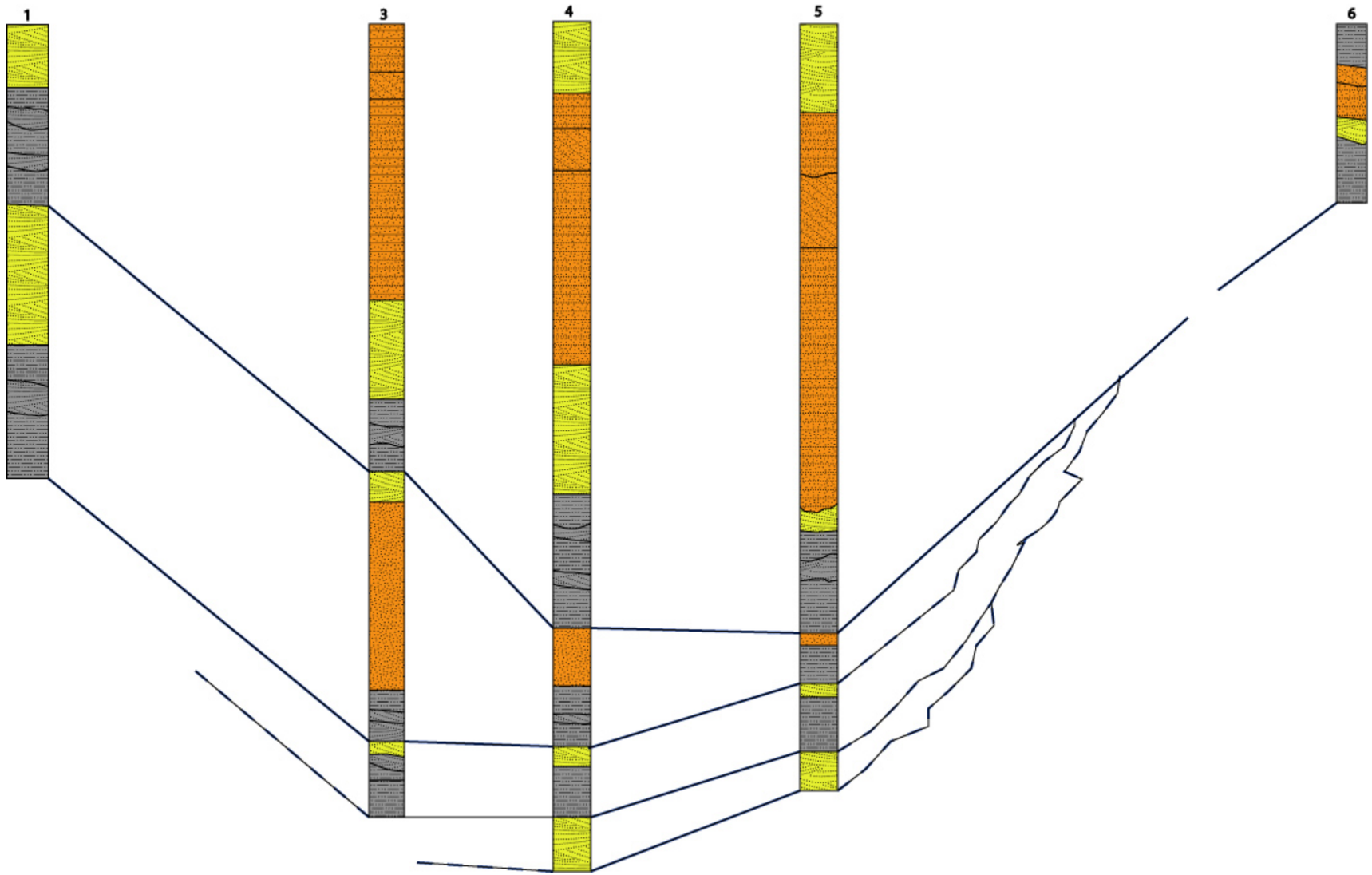

Figure 27 South to North fence diagram with correlation of parasequences found in the Emery Sandstone. Blue lines represent marine flooding surfaces, dashed lines are inferred flooding surfaces. The top parasequence is the most prominent and thickens in the middle of the Wattis Quadrangle, filling in a low on the seabed. All the parasequences pinch out northward and are covered southward. Gray represents the distal lower shoreface composed of deepwater muds and a few hummocks. Yellow represents proximal lower shoreface comprised of amalgamated hummocks and has some bioturbation. Orange represents turbidites comprising of Bauma C and D bedding with the tops having unidirectional flow.

Star Point Sandstone

Panther Tongue at Service Bay Canyon

The Panther Tongue is the lowest sandstone body of the Star Point Sandstone. The sands in the Panther Tongue Member of the Star Point Sandstone thin northward (Figure 28), and are thickest in Service Bay Canyon. This area could have been a topographic low and allowed for the greatest amount of sediment accumulation. In First Canyon, the Panther Tongue Member shows two marine flooding surfaces, whereas Second Water Canyon and Service Bay Canyons exhibit five marine flooding surfaces. The depositional environment of the lowest part of the Panther Tongue Member is the distal lower shoreface throughout the quadrangle, with predominant sandy mudstone and occasional hummocks. These grades vertically into the proximal lower shoreface consisting of amalgamated hummocks. Lying directly on top of the proximal lower shoreface is a 12 m section where no bedding is apparent, as the sand is massive. This section exhibits some bioturbation, and represents the middle shoreface. This is overlain by ~1m of laminar beds, of the upper shoreface. A autocyclic parasequence boundary possibly due to local lobe switching is marked by the laminar beds being overlain by 2 m of TCS bedding of the middle shoreface, which transition into the ~ 1 m thick laminar beds of the upper shoreface. These laminar beds grade into a 3 m thick highly bioturbated section, with *Ophiomorpha* being the predominant trace fossil. The top of this section is marked by a marine flooding event, which represents a second autocyclic parasequence boundary marked by the deepening of the water where the bioturbated section is overlain by a sandy mudstone that has a few hummocks interspersed within it, representing the

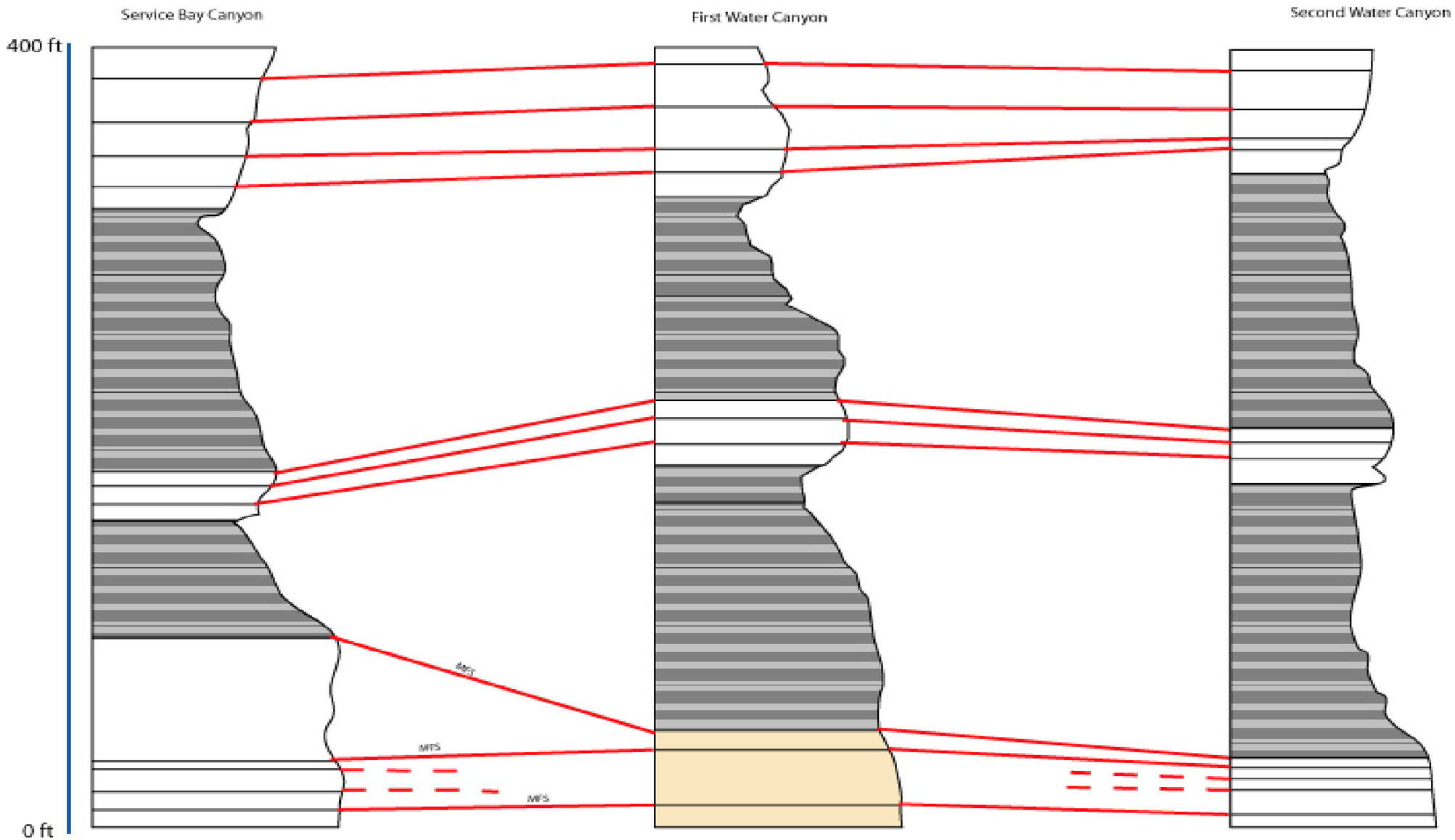

Figure 28. Three parasequence sets of the Star Point Sandstone. The lower parasequence set (Panther Tongue Member Member) is thickest Service Bay Canyon and thins to the north. The second sandstone body thickens in First Water Canyon and is thinner in Service Bay and Second Water Canyon. The final parasequence set is slightly thicker in Service Bay Canyon and thins slightly to the north.

distal lower shoreface. This distal lower shoreface is overlain by a 5 m thick package of amalgamated hummocks with little bioturbation, representing the proximal lower shoreface. The surface of the amalgamated hummock is marked by an exposure surface in this area with small cavities and rhizoids. This surface, if regionally extensive, would represent a sequence boundary on the top of the Panther Tongue Member.

Storres Member at Service Bay Canyon

The Storres Member of the Star Point Sandstone in Service Bay Canyon is composed of three wave-dominated parasequences. The lowest parasequence includes 12 m of distal lower shoreface mudstones, with some hummocky cross stratification, which directly overlie the Panther Tongue Member Member. The distal lower shoreface grades into a 2 m thick section of amalgamated hummocks with some bioturbation. This section represents the proximal lower shoreface. Lying above the proximal lower shoreface is a 1 m thick section of distal lower shoreface of the second parasequence in the Storres Member. This grades into 5 m of amalgamated hummocks of the proximal lower shoreface. Directly above the second proximal lower shoreface is the third parasequence boundary of the Storres Member represented by the deposition of 2.5 m of distal lower shoreface sandy mudstones. These sandy mudstones grade into 5 m of amalgamated hummocks. These amalgamated hummocks represent the upper boundary of the Storres Member parasequence set.

Spring Canyon Member at Service Bay Canyon

The Spring Canyon Member contains five wave dominated parasequences in Service Bay Canyon and these parasequences are grouped together in the third parasequence set of the Star Point Sandstone. The base of the Spring Canyon Member of the Star Point Sandstone includes the 23 m of shale that represents the marine flooding event between the Storres and Spring Canyon Members. This marine flooding event is preserved in the distal lower shoreface that transitions into the amalgamated hummocks of the proximal lower shoreface. The proximal lower shoreface transitions into trough cross stratification of the middle shoreface, followed by a marine flooding event that bounds the first parasequence.

The second parasequence begins with the marine flooding event that produced some reworking of the upper sand in the middle shoreface. These reworked sands transition into the distal lower shoreface composed of shale, with limited hummocks. The distal lower shoreface transitions into the proximal lower shoreface with 2 m of laminar bedding and amalgamated hummocks which are ~3 m thick. Above the proximal lower shoreface is 3 m of multi-directional trough cross stratification and scoured channels filled with cross-bedded sands. The middle shoreface grades to foreshore sands that are 1 m thick and have chiefly laminar bedding that formerly dipped seaward about 2 degrees. A marine flooding surface is located above these foreshore sands.

The third and fourth parasequences are rather similar to the second parasequence, however the fifth parasequence presents significant differences. The fifth parasequence begins in the proximal lower shoreface with amalgamated hummocks, and quickly transitions to middle shoreface sands. The middle shoreface is represented by 1.5 m thick

multidirectional cross-bedded sands and channel sands, with no bioturbation. The middle shoreface grades into the upper shoreface, which is 3 m thick. The lower upper shoreface contains coarse grained sands with laminar to trough cross bedding. These sands grade into foreshore sands that are all laminar bedded with some bioturbation. These sands formerly dipped seaward about 1 degree. The foreshore sands are directly below the first coal seam, which is the boundary between the Spring Canyon Member of the Star Point Sandstone and the Blackhawk Formation. The Spring Canyon Member in Service Bay Canyon is shown in Figure 29.

First Water Canyon

The Panther Tongue Member in First Water Canyon is thinner than that of Service Bay Canyon, having a thickness of only 12 m. Similar to Service Bay Canyon, the parasequence set starts in the distal lower shoreface with mudstone and occasional hummocks within the mudstone. This is overlain by amalgamated hummocks of the proximal lower shoreface that are 0.3 m thick, which, in turn, are overlain by TCS bedded sands representing the middle shoreface. Above the TCS bedded sandstones is a thin layer of laminar beds which only 0.5 m thick that represents the upper shoreface, overlain by a marine flooding surface with the water deepening to the depth of proximal lower shoreface that is represented by 1.5 m thick amalgamated hummocky cross stratification. The middle shoreface is represented by a 3 m bioturbated sandstone grading into the bioturbated zone is a .3 m TCS zone of bedding. The upper shoreface begins with a zone of bioturbation that is 0.5 m thick which, is overlain by laminar beds. This is the top of the second parasequence in First Water Canyon. The water depth then deepened where there is 1 m of mudstone and hummocky cross stratification that grades

Figure 29. Parasequences of the Spring Canyon Member Star Point Sandstone, in Service Bay Canyon. This figure shows long profile of parasequences 2-4.

into amalgamated hummocks of the lower shoreface. The lower shoreface transitions into .7 m of TCS bedding of the middle shoreface, which is the top of the Panther Tongue Member parasequence set.

Second Water Canyon

The base of the Panther Tongue in Second Water Canyon begins in the distal lower shoreface with mudstones and some hummocks. This is overlain by amalgamated hummocks of the proximal lower shoreface and is 1.5 m thick. The next package of sediment is a 3 m highly bioturbated zone that is then overlain with 2.5 m of TCS. Small packages of laminar beds lie on top of the TCS, which is only .5 m thick. A marine flooding surface and the next section of sandstone is composed of amalgamated hummocks from the proximal lower shoreface. The amalgamated hummock section is 1.25 m thick. Once again the amalgamated hummocks are overlain with TCS of the middle shoreface, and then these beds become highly bioturbated and make up 4m worth of sandstone. Small 1 m thick laminar bedding most likely from the upper shoreface marks the end to the shallowing of the sea at this time. Then there was a deepening of the water and .5 m of TCS bedded sandstone was deposited. This TCS grades into bioturbated sandstone that looks like it has some laminar bedding and is 1.5 m thick. This is the top of the parasequence set for the Panther Tongue in Second Water Canyon.

Conclusions

Emery Sandstone

The Emery Sandstone is a series of storm relaxation density currents, deposited in the proximal lower shoreface. The sediment goes from sandy shale to amalgamated

hummocks, then three large sand packages. These large sand packages have hummocks at the tops of them representing the next storms stirring up the sediment, with and there are also sandy mudstones with hummocks in them between the sands. These sand packages are not laterally extensive in the east west direction, but are quite laterally extensive in the northward direction. The Emery Sandstone in the Wattis Quadrangle never got shallower than the proximal lower shoreface.

Star Point Sandstone

These sands are three parasequence sets which represent three major regressions of the Cretaceous Interior Seaway in which the fluvial systems prograded into basin. Only the top parasequence set, and only the last parasequence, get to the beach sands in the upper shoreface, the other parasequences get to the upper shoreface but, never past the lower upper shoreface. The parasequences are fluvial dominated systems (Demko, 2003), and can be used for analogs the deposition of the Mississippi River delta, and the Mahakam river delta of Indonesia.

Bibliography

Allis, R.G., Chidsey, T., Gwynn, W., Morgan, C., White, S., Adams, M., Moore, J., 2002, Natural CO_2 Reservoirs on the Colorado Plateau and Southern Rocky Mountains: Candidates for CO_2 Sequestration: Utah Geological Society, 1-19.

Black, B.J., 2000, Fluid Flow Characterization of the Castlegate Sandstone, Southern Wasatch Plateau, Utah: Interpretation of Reservoir Partitioning Through Permeability and Porosity Analysis: Master's Thesis, Department of Geology, Brigham Young University, p.

BLM, 2002 open file report

BLM, 2005, Coal Report Price Field Office Resource Management Plan Appendix 25, http://www.pricermp.com/documents/Appendicies/Appendix_25-Coal_Report_for_Carbon_and_Emery_Counties.pdf

Bills, T. L., 2000, Groundwater Flow Systems in the Star Point Sandstone, Wasatch Plateau, Utah: Master's Thesis, Department of Geology, Brigham Young University, p.172.

Boggs, S., Jr., 1995, Principles of Sedimentology and Stratigraphy, second edition: Prentice-Hall, New Jersy, p.515-519.

Burns, T.D., and Lamarre, R.A., 1997, Dunkards Wash project: Coalbed methane production from Ferron coals in the east-central Utah, in University of Alabama 1997 International Coalbed Methane Symposium Proceedings Volume, p 507-520.

Carroll, R.E, 1987, Geology of the Standardville 7.5' Quadrangle. Carbon County, Utah, Brigham Young University Geology Studies, V.34, Part 1, p.1-31.

Clark I., Fritz, p., 1997, Environmental Isotopes in Hydrogeology, Lewis Publishers, New York, p. 328.

Cobban, W.A., Merewether, E.A., Fouch, T.D., and Obradovich, J.D., 1994, Some Cretaceous Shorelines in the Western Interior of the United States: Mesozoic Systems of the rocky mountain region, USA, Caputo, M.V., Peterson, J.A., Franczyk, K.J., editors, p. 393-414.

Cross, T.A., 1988, Controls on coal distribution in transgressive-regressive cycles, Upper Cretaceous, Western Interion, USA, in Wilgus, C.K., Hasting, B.S., ST.C. Kendall, C.G., Posamentier, H.W., Ross, C.A., and Van Wagoner, J.C., eds., Sea Level changes: an intergrated approach: SEPM, Special Publication 42, p 371-380.

Demko, T., 2003, Sequence Stratigraphy of the Book Cliffs and Ferron Sandstone field class held at Brigham Young University 2003.

Dewey, J.A., 1997, Facies Analysis, Sequence Stratigraphy, and Depositional History of a Portion of the Ferron Sandstone, Indian Canyon, East-Central Utah: Master's Thesis, Department of Geology, Brigham Young University.

Doelling, H.H., 1972, Central Utah coal fields-Sevier-Sanpete, Wasatch Plateau, Book Cliffs, and Emery: Utah Geological and Mineralogical Survey Monograph 3, p. 572.

Doelling, H.H., Smith, M.R., 1982, Overview of Utah coal fields, 1982 in Gugel, K.D., editor, Proceedings of the Fifth Symposium on the Geology of Rocky Mountain Coal: Utah geological and Mineral Survey Bulletin 118, p. 1-26.

Dyman, T.S., Merewether, E.A., Molenaar, C.M., Cobban, W.A., Obradovich, J.D., Weimer, R.J., and Bryant, W.A., 1994, Stratigraphic transects for Cretaceous rocks, rocky mountain and Great Plains regions, Mesozoic Systems of the Rocky Mountain Region, USA, Society of Sedimentary Geology Rocky Mountain Section, Caputo, M.V., Peterson, J.A., Franczyk, KJ., editors, p. 365-392.

Edwards, C.M., Howell, J.A., Flint, S.S., 2001, Sratigraphic Evidence for Episodic Partitioning of the Western Interior Basin, Utah, BSRG, University of Plymouth.

Edwards, C.M., Howell, J.A., Flint, S.S., 2003, Controls on the Depositional Patterns in the Santonian Emery Sandstone Member and Surrounding Strata, Wasatch Plateau, Utah, Department of Earth Sciences, Stratigraphy Research Group, University of Liverpool: AAPG Annual Meeting 2003.

Elder, W. P., Kirkland, J. I., 1994, Cretaceous Paleogeography of the Southern Western Interior Region, in Mesozoic Systems of the Rocky Mountain Region, USA, Society for Sedimentary Geology Rocky Mountain Section, Caputo, M.V., Peterson, J.A., Franczyk, KJ., editors p. 415-440.

Environmental Isotopes Laboratory, 1998, Tritium Analysis: Technical Pricedure 1.0, Department of Earth Sciences, University of Waterloo.

EPA, 1983, Methods for chemical analysis of water and wastes-EPA-600 4-79-020: National Exposure Research Laboratory, Cincinnati, Ohio.

Flores, R.M., Blanchard, L.F., Sanchez, J.D., Marley, W.E., Muldoon, W.J., 1984, Paleogeographic controls of coal accumulation, Cretaceous Blackhawk Formation and Star Point Sandstone, Wasatch Plateau, Utah: AAPG Bulletin v 95/5. p. 540-550.

Gardner, M.H., Cross, T.A., 1994, Middles Cretaceous Paleogeography of Utah, Mesozoic Systems of the Rocky Mountain Region, USA, Caputo, M.V., Peterson, J.A., Franczyk, K.J., editors, p. 471-502.

Gibbs, T.D.,1998, Constraints of Sedimentology, stratigraphy, and structure on conceptual models of subsurface flow pathways of springs in the Wasatch Plateau and Book Cliffs, Utah: Master's Thesis, Department of Geology, Brigham Young University, p.68.

Gloyn, R.W., et al., 2003, Energy, mineral, and ground-water resources of Carbon and Emery Counties, Utah: Utah Geological Survey, Bulletin 132, p. 167.

Hansen, C.D., 1988, Geology of the Jump Creek 7.5 ' Quadrangle Carbon County, Utah: Masters Thesis, Department of Geology, Brigham Young University, p.70.

Hintze, L.F., 1988, Geologic history of Utah, Brigham Young University Special Publication 7, p. 53-200.

Hintze L.F., 1993, Geological Map of the State of Utah.

Holman, L.S., 2001, The effect of parasequence geometry and facies architecture on reservoir partitioning of the star point sandstone, Wasatch Plateau, Utah: Master's Thesis, Department of Geology, Brigham Young University, p 8-12,51-57,138-157 .

Lawton, T.F., 1994, Tetonic Setting of Mesozoic Sedimentary Basins, Rocky Mountain Region, United States, , in Mesozoic Systems of the Rocky Mountain Region, USA, Society for Sedimentary Geology Rocky Mountain Section, Caputo, M.V., Peterson, J.A., Franczyk, KJ., editors p. 1-26.

Knowles, S.P., 1985, Geology of the Scofield 7.5 Minute Quadrangle in Carbon, Emery, and Sanpete Counties, Utah: Brigham Young University Geology Studies, V. 32, Part 1, p.85-100.

Mayo A.L., Morris, T.H., et al., 2004, Active and inactive groundwater flow systems: Evidence from a stratified, mountainous terrain: GSA Bulletin, p. 1456-1472.

Matheny, J. P., and Picard, M. D., 1985, Sedimentology and depositional environments of the Emery Sandstone Member of the Mancos Shale, Emery and Sevier Counties, Utah: AAPG Bulletin v. 22, no. 3, p. 94-109.

McCrea, J.M., 1950, On the isotopic chemisty of carbonates and a paleotemperature scale: Journal of Physical Chemistry, v. 18, pp. 849-857.

Mitchum, R.M., Vail, P.R., and Thompson, S. III, 1977, Seismic stratigraphy and global changes of sea level, part 2 the depositional sequence as a basic unit for

stratigraphic analysis, in C.E. Payton, ed., Seismic Stratigraphy applications to hydrocarbon exploration: AAPG Memoir 26, p. 53-62.

Montgomery, S.L., Tabet, D.E., and Barker, C.E., Upper Cretaceous Ferron Sandstone: Major coalbed methane play in central Utah: AAPG Bulletin v.85, p. 199-219

Nelson, S.T., and Dettman, D., 2001, Improving hydrogen isotope ratio measurements for on-line Cr reduction systems: Rapid Communications in Mass Spectrometry, v. 15, p 2301-2306.

Nelson, S.T., 2000, A simple, practical methodology for routine VSMOW/SLAP normalization of Water Samples Analyzed by Continuous Flow Methods: Rapid Communications in Mass Spectrometry, v. 14, p. 1044-1046.

Nethercott, M.A., 1986, Geology of the Deadman Canyon 7.5 Minute Quadrangle, Carbon County, Utah: Brigham Young University Geology Studies, V. 33, Part 1, p.45-86.

Pfaff, J.D., Brockhoff, C.A., and O'Dell, J.W., 1991, EPA Test Method: The determination of inorganic anions in water by ion chromatography-Method 300.0: National Exposure Research Laboratory, Cincinnati, Ohio.

Prothero, D.R., 1990, Interpreting the Stratigraphic Record: W.H. Freeman and Company, p. 113-114.

Sahagian, D., Proussevitch, A., and Carlson, W., 2002, Timing of Colorado Plateau uplift: Initial constraints from vesicular basalt-derived paleoelevations: Geology, v. 30, no. 9, p. 807-810.

Spieker, E.M. and Reeside, J.B., Jr., 1925, Cretaceous and Tertiary formations of the Wasatch Plateau, Utah: Geological Society of America Bulletin, v. 36, no. 3, p. 435-454.

Spieker, E.M., 1931, The Wasatch Plateau Coal Field Utah: United States Geologic Society Bulletin 819, p 1- 232.

Spieker, E.M., 1949, The Transition Between the Colorado Plateaus and the Great Basin in Central Utah: Guidebook to the Geology of Utah number 4, Utah Geological Society, p. 1-106.

Strack, D., 2001, Utah Fuels the West, Utah's coal industry and the railroads that served it, Wattis Mine: http://utahrails.net/utahcoal/utahcoal-wattis.php

Tabet, D.E., Quick, J.P., and Sommer, S.N., 1995a, The resinite resources of selected coal seams of the Book Cliffs and Wasatch Plateau coal fields of central Utah: Utah Geological Survey Report of Investigation 225, p. 19.

Taylor, D.R., and Lovell, R.W.W., 1995 High-Frequency Sequence Stratigraphy and Paleogeography of the Kenilworth Member, Blackhawk Formation, Book Cliffs, Utah, U.S.A. in Sequence Stratigraphy of Foreland Basin Deposits: Outcrop and Subsurface Examples from the Cretaceous of North America , van Wagoner, J.C., and Bertram, G.T., ed.: AAPG Memoir 64, pp. 257-275.

Tripp, C.N., 1989, A hydrocarbon exploration model for the Cretaceous Ferron Sandstone Member of the Mancos Shale, and the Dakota Group in the Wasatch Plateau and Castle Valley of east-central Utah, with emphasis on post-1980 subsurface data: Utah Geological Surbey Open-File Report 160, p. 81 paltes, scale 1:24000.

Tingey, D.G., 1989, Late Oligocene and Miocene Minette and Olivine Nephelinte Dikes, Wasatch Plateau, Utah: Master's Thesis, Department of Geology, Brigham Young University, p. 75.

Tingey, D.G., 2005, Personal Comunication on the location of faults in the Cyprus Plateau Coal Mine.

USGS, 2005, Utah's Sevier Thrust System: http://geology.utah.gov/utahgeo/geo /thrustfault5.htm

Willis, G., Doelling, H.H., 1995, Guide to authors of geologic maps and text booklets of the Utah Geological Survey: UGS, p.98

Witkind, I.J., Weiss, M.P., and Brown, T.L., 1987 Geologic map of the Manti 30'x60' Quadrangle, Carbon, Emery, Grand, and Uintah Counties, Utah: U.S. Geological Survey Miscellaneous Investigations Series Map 1-1764 scale 1:100,000.

Witkind, I.J., 1995 Geologic map of the Price 1° x 2° Quadrangle, Utah: U.S. Geologic Survey Miscellaneous Investigations Series Map 1-2462, scale 1:250,000.

Van de Graff, F.R., 1972, Fluvial-deltaic facies of the Castlegate Sandstone (Cretaceous) east-central Utah: Journal of Sedimentary Petrology, v. 42, no. 3 p. 558-571.

Van Sant, J.N., 1964, Refactory-clay deposits of Utah: U.S. Bureau of Mines Information Circular 8313 p. 84-89.

van Wagoner, J. C., H. W. Posamentier, R. M. Mitchum, P. R. Vail, J. F. Sarg, T. S. Loutit, and J. Hardenbol, 1988, An overview of the fundamentals of sequence stratigraphy, in C. K. Wilgus, and a. others, eds., Sea-Level Change: An Integrated Approach, SEPM Special Publication 42, p. 39-45.

van Wagoner, J.C., Mitchum, R.M., Campion, K.M., and Rahmanian, V.D., 1990, Siliciclastic sequence stratigraphy in well logs, cores, and outcrops: Concepts for

high-resolution correlation of time and facies: Houston, Texas: American Association of Petroleum Geologists Methods in Exploration Series, v. 42, p. 558–571.

van Wagoner, J.C., Bertram, G.T., 1995, Sequence Stratigraphy of foreland Basin Deposits: AAPG Memoir 64, p. 490.

Zentner, M.A., 2001, Timing and Mechanisms of Groundwater Recharge in a Mountainous Terrain of a Temperate Climate: Mater's Thesis, Department of Geology, Brigham Young University, p.104.

Appendix A
Solute Data

Solute Data
Wattis UT 7.5' Quadrangle

Lab #	Field Name	Date Collected	Formation		mg/L															0.05	0.0823
				pH	Ca	Mg	Na	K	Fe	Mn	Sr	HCO_3	CO3	F	Cl	NO_2	NO3	Br	HPO_4	SO_4	Ca	Mg
2771	Spring 2	5/8/2002	North Horn	7.09	60.69	13.87	1.99	1.77	0.01	0.108		241.1	0	0.09	1.365	0	0.127	0	0	8.714	3.03	1.14
2772	Spring 3	5/8/2002	North Horn	6.71	51.11	5.06	1.04	1.42	0.01	0.108	0	176.2	0	0.23	0.87	0	1.9	0	0	2.127	2.55	0.42
2770	Spring 1	5/8/2002	North Horn	6.86	58.49	12.98	3.01	1.19	0.05	0.01	0	248	0	0.07	2.973	0	0.49	0	0.12	12.57	2.92	1.07
2773	Spring 4	5/8/2002	North Horn	6.66	51.93	22.78	1.21	0.95	0.04	0.01	0	278	0	0.08	1.43	0	1.5	0	0.12	2.53	2.59	1.87
2980	Mohrland	5/13/2002	Blackhawk	6.77	125.4	57.18	6.26	4.6	0.11	0	0	438.3	0	0.11	3.85	0	0.14	0	0	208.4	6.26	4.71
3079	Mohrland	9/30/2002	Blackhawk	7.11	126.6	56.13	6.09	4.47	0.03	0.02	0	457.66	0	0	3.85	0	0.141	0	0	209.8	6.32	4.62
3080	Spring 1	9/30/2002	North Horn	7.49	60.32	11.57	2.72	0.92	0.02	0.11	0	254.06	0	0.05	2.55	0	0	0	0	9.798	3.01	0.95
3081	Spring 2	9/30/2002	North Horn	7.76	87.63	14.66	2.52	2.85	0.03	0.113		351.2	0	0.164	1.686	0	1.175	0		13.22	4.37	1.21
3082	Spring 3	9/30/2002	North Horn	7.52	71.38	8.64	1.12	0.99	0.03	0.115		268.24	0	0.187	1.02	0	0.558	0	0	1.67	3.56	0.71
3083	Spring 4	3/30/2002	North Horn	7.4	47.58	24.01	1.31	0.29	0.04	0.02	0	277.84	0	0.06	1.38	0	2.07	0	0	2.55	2.37	1.98
3733	First Water Spring 3	5/29/2004	Star Point	7.6	33.73	10.32	11.44	2.65	0.53			160.2		3.763	5.494					9.419	1.68	0.85
3734	First Water Spring 5	5/29/2004	Star Point	7.3	3.51	0.52	2.16	1.34	0.35			16.9		0.521	1.456					0	0.18	0.04
3735	First Water Spring 2	5/29/2004	Star Point	7.4	27.3	2.14	6.48	2.19	0.61			106.2		0.428	1.781		10.8	1.3		1.975	1.36	0.18
3736	First Water Spring 4	5/29/2004	Star Point	7.1	19.98	3.231	6.38	1.24	0.2			91.1		2.541	2.439	0	0			2.599	1	0.27
3737	First Water Spring 7	5/29/2004	Star Point	7.3	26.35	2.67	5.65	1.14	1.04			102.5		0.474	0.609		0.318			1.541	1.31	0.22
3738	First Water Spring 1	5/29/2004	Star Point	7.2	22.08	1.86	5.19	0.86	1.17			91		0.47	0.475		0			4.105	1.1	0.15

Solute Data

Lab #	Field Name	0.0435 Na	0.0256 K	0.0537 Fe	0.023 Sr	0.016 HCO3	0.0333 CO3	0.053 F	0.0282 Cl	0.016 NO2	0.0161 NO3	0.013 Br	0.021 HPO4	0.0208 SO4	Si	total cations	total anions	% error
2771	Spring 2	0.09	0.05	0.00	0.00	3.95	0.00	0.00	0.04	0.00	0.00	0.00	0.00	0.18		4.31	4.17	1.70
2772	Spring 3	0.05	0.04	0.00	0.00	2.89	0.00	0.01	0.02	0.00	0.03	0.00	0.00	0.04		3.06	2.99	1.20
2770	Spring 1	0.13	0.03	0.00	0.00	4.06	0.00	0.00	0.08	0.00	0.01	0.00	0.00	0.26		4.15	4.41	-3.00
2773	Spring 4	0.05	0.02	0.00	0.00	4.56	0.00	0.00	0.04	0.00	0.02	0.00	0.00	0.05		4.53	4.67	-1.50
2980	Mohrland	0.27	0.12	0.01	0.00	7.18	0.00	0.01	0.11	0.00	0.00	0.00	0.00	4.34		11.37	11.64	-1.20
3079	Mohrland	0.26	0.11	0.00	0.00	7.50	0.00	0.00	0.11	0.00	0.00	0.00	0.00	4.37		11.31	11.98	-2.90
3080	Spring 1	0.12	0.02	0.00	0.00	4.16	0.00	0.00	0.07	0.00	0.00	0.00	0.00	0.20		4.10	4.43	-3.90
3081	Spring 2	0.11	0.07	0.00	0.00	5.76	0.00	0.01	0.05	0.00	0.02	0.00	0.00	0.28		5.76	6.12	-3.00
3082	Spring 3	0.05	0.03	0.00	0.00	4.40	0.00	0.01	0.03	0.00	0.01	0.00	0.00	0.03		4.35	4.48	-1.50
3083	Spring 4	0.06	0.01	0.00	0.00	4.55	0.00	0.00	0.04	0.00	0.03	0.00	0.00	0.05		4.42	4.67	-2.80
3733	First Water Spring 3	0.50	0.07	0.03	0.00	2.63	0.00	0.20	0.15	0.00	0.00	0.00	0.00	0.20		3.13	3.18	-0.80
3734	First Water Spring 5	0.09	0.03	0.02	0.00	0.28	0.00	0.03	0.04	0.00	0.00	0.00	0.00	0.00		0.36	0.35	1.40
3735	First Water Spring 2	0.28	0.06	0.03	0.00	1.74	0.00	0.02	0.05	0.00	0.17	0.02	0.00	0.04		1.91	2.04	-3.30
3736	First Water Spring 4	0.28	0.03	0.01	0.00	1.49	0.00	0.13	0.07	0.00	0.00	0.00	0.00	0.05		1.59	1.74	-4.50
3737	First Water Spring 7	0.25	0.03	0.06	0.00	1.68	0.00	0.02	0.02	0.00	0.01	0.00	0.00	0.03		1.87	1.76	3.00
3738	First Water Spring 1	0.23	0.02	0.06	0.00	1.49	0.00	0.02	0.01	0.00	0.00	0.00	0.00	0.09		1.56	1.61	-1.60

Appendix B
Stable Isotopes

Stable Isotopes
Wattis Quadrangle, Carbon and Emery Counties, Utah

Sample ID	Filed Name	Formation	Date Collected	δ^2H (‰)	+/-	$\delta^{18}O$ (‰)	+/-
2770	Spring 1	North Horn	5/8/2002	-123.1	1	-16.78	0.21
2771	Spring 2	North Horn	5/8/2002	-118.7	1	-16.45	0.21
2772	Spring 3	North Horn	5/8/2002	-121.7	1	-16.44	0.21
2773	Spring 4	North Horn	5/8/2002	-121.2	1	-16.69	0.21
2980	Morhland	Blackhawk	5/13/2002	-124.0	1	-16.68	0.21
3079	Morhland	Blackhawk	9/30/2002	-124.0	1	-16.61	0.21
3080	Spring 1	North Horn	9/30/2002	-123.2	1	-16.90	0.21
3081	Spring 2	North Horn	9/30/2002	-119.1	1	-16.29	0.21
3082	Spring 3	North Horn	9/30/2002	-120.1	1	-16.47	0.21
3083	Spring 4	North Horn	9/30/2002	-122.4	1	-16.89	0.21
3733	First Water Canyon Spring 3	Star Point	5/29/2004	-118.8	1	-16.29	0.09
3734	First Water Canyon Spring 5	Star Point	5/29/2004	-123.6	1	-16.87	0.09
3735	First Water Canyon Spring 2	Star Point	5/29/2005	-120.0	1	-15.92	0.09
3736	First Water Canyon Spring 4	Star Point	5/29/2005	-123.5	1	-17.03	0.09
3737	First Water Canyon Spring 7	Star Point	5/29/2005	-120.5	1	-16.14	0.09
3738	First Water Canyon Spring 1	Star Point	5/29/2005	-128.5	1	-17.10	0.09

Appendix C
Radi-Isotope Data

Wattis UT 7.5' Quadrangle

Sample Id	Field Name	Formation	sample date	pH	temp	pmc	δ13C	TU	±	Age
2980	Morhland	Blackhawk	5/13/2002	6.77	10	19	11	2.1	0.19	10000±500
3079	Morhland	Blackhawk	9/30/2002	7.11	15	24.8	10.6	4.02	0.3	7100±500
3738	First Water Canyon Spring 1	Star Point	5/29/2004	7.2	2.30	40.3	-10.56	4.99	0.18	3200±300
2771	Spring 2	North Horn	5/8/2002	8	3.1	103		8.24	0.28	Modern
2772	Spring 3	North Horn	5/8/2002	7.7	4.1			5.04	0.21	Modern
2770	Spring 1	North Horn	5/8/2002	8.2	7.6	102		8.18	0.21	Modern
3080	Spring 1	North Horn	9/30/2002	7.49	6			6.13	0.22	Modern
3081	Spring 2	North Horn	9/30/2002	7.76	8			6.17	0.2	Modern
3082	Spring 3	North Horn	9/30/2002	7.52	10.3			9.82	0.36	Modern
3083	Spring 4	North Horn	9/30/2002	7.4	3			11.5	0.29	Modern
2773	Spring 4	North Horn	5/8/2002	7.9	3			5.94	0.18	Modern
3733	First Water Canyon Spring 3	Star Point	5/29/2004	7.6	3.7			9.6	0.3	Modern
3734	First Water Canyon Spring 5	Star Point	5/29/2004	7.3	2.8	102.8		7.23	0.3	Modern
3735	First Water Canyon Spring 2	Star Point	5/29/2004	7.4	3.2			7.6	0.3	Modern
3736	First Water Canyon Spring 4	Star Point	5/29/2004	7.1	3.4			7.6	0.3	Modern
3737	First Water Canyon Spring 7	Star Point	5/29/2004	7.3	4.5	99.1		7.9	0.3	Modern

Appendix D
Statistical Analysis

			Date Collected	Formation			mg/L							
	Lab #	Field Name			Temp °C	pH	Ca	Mg	Na	K	Fe	Mn	Sr	HCO3
	2771	Spring 2	5/8/2002	North Horn	3.1	8	60.69	13.87	1.99	1.77	0.008	0.108		241.1
KTNh	2772	Spring 3	5/8/2002	North Horn	4.1	7.7	51.11	5.06	1.04	1.42	0.013	0.108	0	176.2
	2770	Spring 1	5/8/2002	North Horn	7.6	8.2	58.49	12.98	3.01	1.19	0.052	0.01	0	248
	2773	Spring 4	5/8/2002	North Horn	3	7.9	51.93	22.78	1.21	0.95	0.036	0.01	0	278
	Average				4.45	7.95	55.555	13.67	1.8125	1.333	0.0273	0.059	0	235.825
	Deviation													
Ttest	Spring vs fall													
	2980	Mohrland		Blackhawk	10	6.767	125.4	57.18	6.26	4.6	0.11	0	0	438.3
Kb	3079	Mohrland	9/30/2002	Blackhawk	15	7.11	126.6	56.13	6.09	4.47	0.03	0.02	0	457.66
	Average				12.5	6.9385	126	56.66	6.175	4.535	0.07	0.01	0	447.98
	Deviation													
Ttest	Kb vs Kbs													
Ttest	Spring vs Kb													
	3080	Spring 1	9/30/2002	North Horn	6	7.49	60.32	11.57	2.72	0.92	0.019	0.11	0	254.06
	3081	Spring 2	9/30/2002	North Horn	8	7.76	87.63	14.66	2.52	2.85	0.032	0.113		351.2
KTnh	3082	Spring 3	9/30/2002	North Horn	10.3	7.52	71.38	8.64	1.12	0.99	0.029	0.115		268.24
	3083	Spring 4	9/30/2002	North Horn	3	7.4	47.58	24.01	1.31	0.29	0.04	0.02	0	277.84
	Average				6.825	7.5425	66.728	14.72	1.9175	1.263	0.03	0.0895	0	287.835
	Deviation													
Ttest	Spring vs Fall													
Starpoint	3733	First Water Canyon Spring 3	5/29/2004	Star Point Sandstone	3.70	7.6	33.73	10.32	11.44	2.65	0.526			160.2
	3734	First Water Canyon Spring 5	5/29/2004	Star Point Sandstone	2.80	7.3	3.51	0.52	2.16	1.34	0.352			16.9
	3735	First Water Canyon Spring 2	5/29/2004	Star Point Sandstone	3.20	7.4	27.3	2.14	6.48	2.19	0.614			106.2
	3736	First Water Canyon Spring 4	5/29/2004	Star Point Sandstone	3.40	7.1	19.98	3.231	6.38	1.24	0.203			91.1
	3737	First Water Canyon Spring 7	5/29/2004	Star Point Sandstone	4.50	7.3	26.35	2.67	5.65	1.14	1.037			102.5
	3738	First Water Canyon Spring 1	5/29/2004	Star Point Sandstone	2.30	7.2	22.08	1.86	5.19	0.86	1.172			91
	Average				3.31667	7.31667	22.158	3.457	6.2167	1.57	0.6507	#DIV/0!	#DIV/0!	94.65
	Deviation													
Ttest	Kbs vs Kb													
Ttest	Spring vs Kbs													

											TDS meq	0.0499 Ca	0.08229 Mg	0.0435 Na
	Lab #	CO3	F	Cl	NO2	NO3	Br	HPO4	SO4	Si				
	2771	0	0.09	1.365	0	0.127	0	0	8.714	0	4.26	3.03	1.14	0.09
KTNh	2772	0	0.23	0.87	0	1.9	0	0	2.127		3.02	2.55	0.42	0.05
	2770	0	0.07	2.973	0	0.49	0	0.12	12.57	0	4.12	2.92	1.07	0.13
	2773	0	0.08	1.43	0	1.5	0	0.12	2.53	0	4.51	2.59	1.87	0.05
	Average	0	0.1175	1.6595	0	1.00425	0	0.06	6.48525	0	3.9775	2.7725	1.125	0.08
	Deviation										0.65840084	0.238659451	0.593099205	0.038297084
Ttest	Spring vs fall										0.23377507	0.25456024	0.8360037	0.85373822
	2980	0	0.11	3.85	0	0.14	0	0	208.42	0	11.24	6.26	4.71	0.27
Kb	3079	0	0	3.85	0	0.141	0	0	209.82	0	11.2	6.32	4.62	0.26
	Average	0	0.055	3.85	0	0.1405	0	0	209.12	0	11.22	6.29	4.665	0.265
	Deviation										0.028284271	0.042426407	0.06363961	0.007071068
Ttest	Kb vs Kbs										6.1278E-06	9.76582E-06	9.15662E-07	0.948300869
Ttest	Spring vs Kb										0.000125889	4.03773E-05	0.001360403	0.00305284
	3080	0	0.05	2.55	0	0	0	0	9.798		4.08	3.01	0.95	0.12
	3081	0	0.164	1.686	0	1.175	0		13.223		5.69	4.37	1.21	0.11
KTnh	3082	0	0.187	1.02	0	0.558	0	0	1.67	0	4.32	3.56	0.71	0.05
	3083	0	0.06	1.38	0	2.07	0	0	2.55	0	4.41	2.37	1.98	0.06
	Average	0	0.11525	1.659	0	0.95075	0	0	6.81025	0	4.625	3.3275	1.2125	0.085
	Deviation										0.723532999	0.848228546	0.550900778	0.035118846
Ttest	Spring vs Fall										0.23377507			
Starpoint	3733		3.763	5.494					9.419		3.03	1.68	0.85	0.5
	3734		0.521	1.456					0		0.31	0.18	0.04	0.09
	3735		0.428	1.781		10.798	1.301		1.975		1.82	1.36	0.18	0.28
	3736		2.541	2.439	0	0			2.599		1.55	1	0.27	0.28
	3737		0.474	0.609		0.318			1.541		1.78	1.31	0.22	0.25
	3738		0.47	0.475		0			4.105		1.48	1.1	0.15	0.23
	Average	#DIV/0!	1.3661667	2.042333	0	2.779	1.301	#DIV/0!	3.27316667	#DIV/0!	1.661666667	1.105	0.285	0.271666667
	Deviation										0.869929116	0.510754344	0.28738476	0.132274966
Ttest	Kbs vs Kb													
Ttest	Spring vs Kbs										0.002001343			

		0.02558	0.05372	0.0228	0.01639	0.033	0.05264	0.02821	0.0161	0.01613	0.01252	0.0208	0.02082		total	total	%
	Lab #	K	Fe	Sr	HCO3	CO3	F	Cl	NO2	NO3	Br	HPO4	SO4	Si	cations	anions	error
	2771	0.05	0	0	3.95	0	0	0.04	0	0	0	0	0.18		4.31	4.17	1.7
KTNh	2772	0.04	0	0	2.89	0	0.01	0.02	0	0.03	0	0	0.04		3.06	2.99	1.2
	2770	0.03	0	0	4.06	0	0	0.08	0	0.01	0	0	0.26		4.15	4.41	-3
	2773	0.02	0	0	4.56	0	0	0.04	0	0.02	0	0	0.05		4.53	4.67	-1.5
	Average	0.035	0	0	3.865	0	0.0025	0.045	0	0.015	0	0	0.1325		4.0125	4.06	-0.4
	Deviation	0.01291	0	0	0.702116	0	0.005	0.025166	0	0.01291	0	0	0.10626				
Ttest	Spring vs fall	0.870098			0.139369		0.536963	0.874816		1			0.92858				
	2980	0.12	0.01	0	7.18	0	0.01	0.11	0	0	0	0	4.34		11.37	11.64	-1.2
Kb	3079	0.11	0	0	7.5	0	0	0.11	0	0	0	0	4.37		11.31	11.98	-2.9
	Average	0.115	0.005	0	7.34	0	0.005	0.11	0	0	0	0	4.355		11.34	11.81	-2.05
	Deviation	0.007071	0.007071	0	0.226274	0	0.007071	0	0	0	0	0	0.02121				
Ttest	Kb vs Kbs	0.002528	0.103437		5.13E-05		0.300659	0.206		0.57933	0.60365		2.5E-10				
Ttest	Spring vs Kb	0.001404	0.177808		0.00291		0.632813	0.026203		0.19626			7.8E-07				
	3080	0.02	0	0	4.16	0	0	0.07	0	0	0	0	0.2		4.1	4.43	-3.9
	3081	0.07	0	0	5.76	0	0.01	0.05	0	0.02	0	0	0.28		5.76	6.12	-3
KTnh	3082	0.03	0	0	4.4	0	0.01	0.03	0	0.01	0	0	0.03		4.35	4.48	-1.5
	3083	0.01	0	0	4.55	0	0	0.04	0	0.03	0	0	0.05		4.42	4.67	-2.8
	Average	0.0325	0	0	4.7175	0	0.005	0.0475	0	0.015	0	0	0.14		4.6575	4.925	-2.8
	Deviation	0.0263	0	0	0.71332	0	0.005774	0.017078	0	0.01291	0	0	0.12028				
Ttest	Spring vs Fall																
Starpoint	3733	0.07	0.03	0	2.63	0	0.2	0.15	0	0	0	0	0.2		3.13	3.18	-0.8
	3734	0.03	0.02	0	0.28	0	0.03	0.04	0	0	0	0	0		0.36	0.35	1.4
	3735	0.06	0.03	0	1.74	0	0.02	0.05	0	0.17	0.02	0	0.04		1.91	2.04	-3.3
	3736	0.03	0.01	0	1.49	0	0.13	0.07	0	0	0	0	0.05		1.59	1.74	-4.5
	3737	0.03	0.06	0	1.68	0	0.02	0.02	0	0.01	0	0	0.03		1.87	1.76	3
	3738	0.02	0.06	0	1.49	0	0.02	0.01	0	0	0	0	0.09		1.56	1.61	-1.6
	Average	0.04	0.035	0	1.551667	0	0.07	0.056667	0	0.03	0.00333	0	0.06833		1.736666667	1.78	-0.966666667
	Deviation	0.02	0.020736	0	0.753589	0	0.076942	0.050465	0	0.0687	0.00816	0	0.07083				
Ttest	Kbs vs Kb																
Ttest	Spring vs Kbs																

Plate 1

UNITED STATES
DEPARTMENT OF THE INTERIOR
GEOLOGICAL SURVEY

STATE OF UTAH
UTAH GEOLOGICAL AND MINERAL SURVEY

WATTIS QUADRANGLE
UTAH
7.5 MINUTE SERIES (TOPOGRAPHIC)

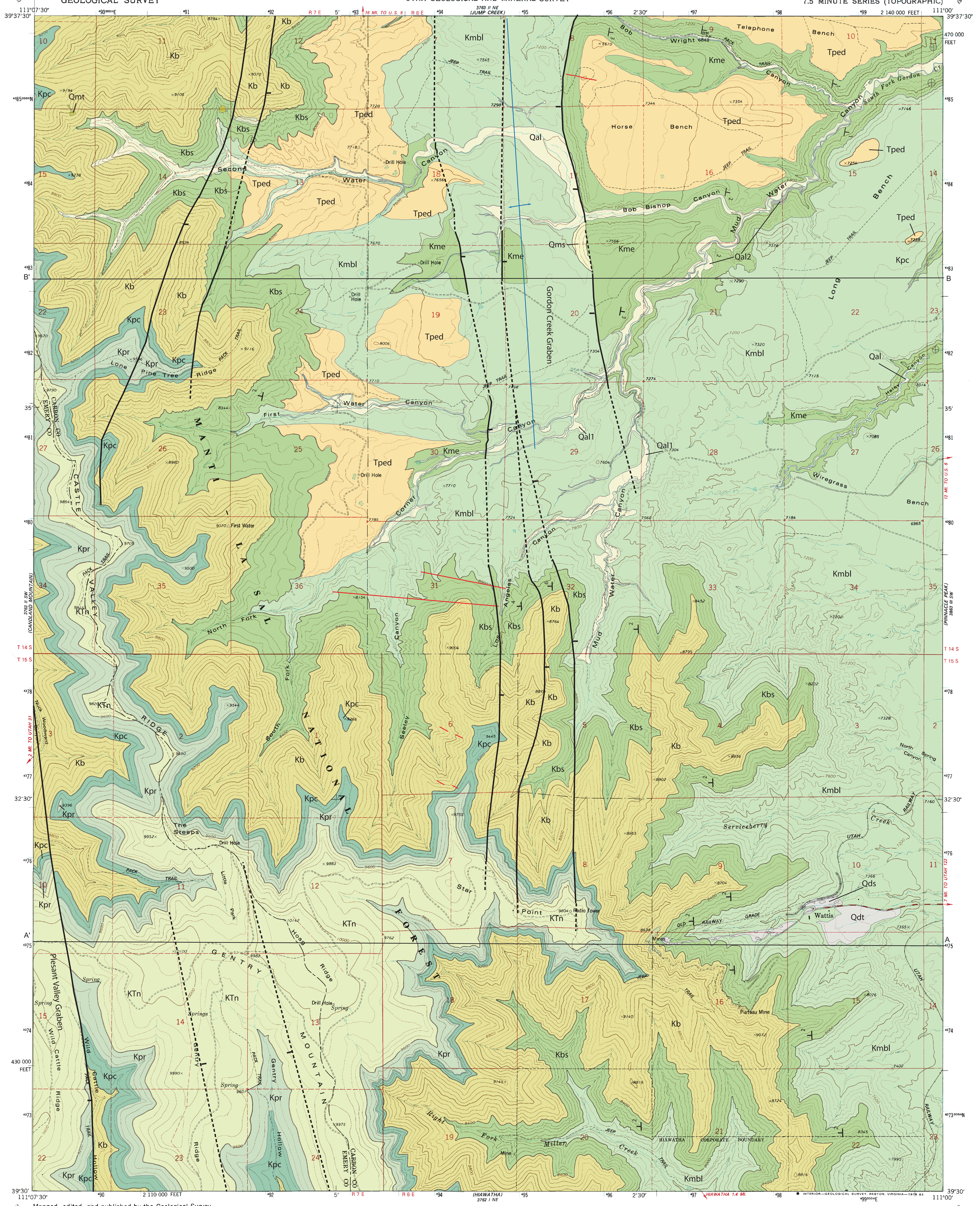

Mapped, edited, and published by the Geological Survey

Control by USGS, NOS/NOAA, and U. S. Forest Serivce

Topography by photogrammetric methods from aerial photographs taken 1970. Field checked 1974. Map edited 1979

Projection and 10,000-foot grid ticks: Utah coordinate system, central zone (Lambert conformal conic) 1000-meter Universal Transverse Mercator grid ticks, zone 12, shown in blue. 1927 North American datum

Fine red dashed lines indicate selected fence lines

There may be private inholdings within the boundaries of the National or State reservations shown on this map

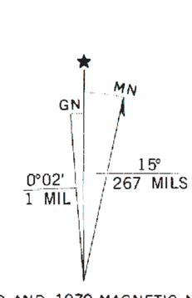

UTM GRID AND 1979 MAGNETIC NORTH DECLINATION AT CENTER OF SHEET

SCALE 1:24 000

CONTOUR INTERVAL 80 FEET
NATIONAL GEODETIC VERTICAL DATUM OF 1929

THIS MAP COMPLIES WITH NATIONAL MAP ACCURACY STANDARDS
FOR SALE BY U. S. GEOLOGICAL SURVEY, DENVER, COLORADO 80225, OR RESTON, VIRGINIA 22092
A FOLDER DESCRIBING TOPOGRAPHIC MAPS AND SYMBOLS IS AVAILABLE ON REQUEST

ROAD CLASSIFICATION

Primary highway, hard surface
Light-duty road, hard or improved surface
Secondary highway, hard surface
Unimproved road
Interstate Route
U. S. Route
State Route

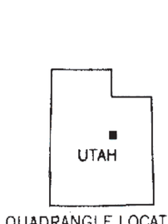

QUADRANGLE LOCATION

WATTIS, UTAH
N3930—W11100/7.5

1979

DMA 3763 II SE—SERIES V897

Strat Column

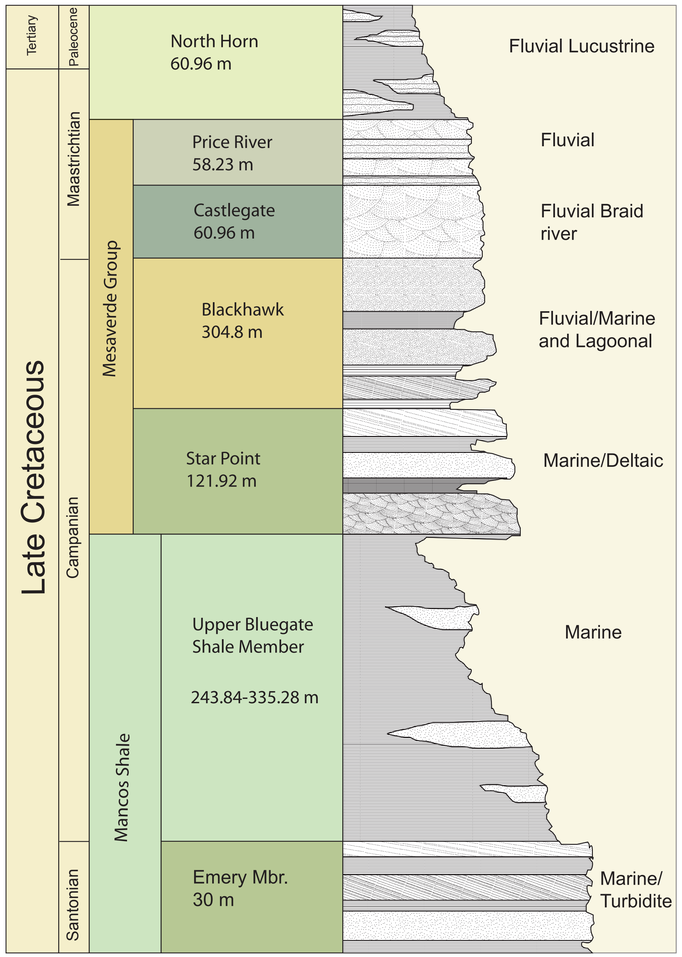

CORRELATION OF MAP UNITS

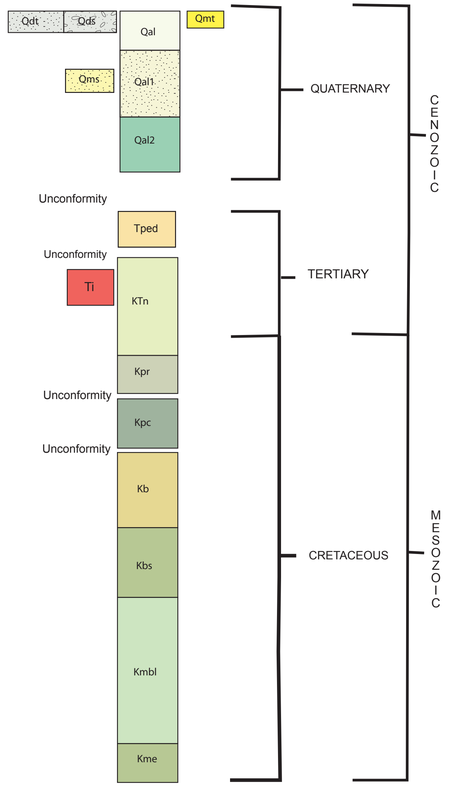

DESCRIPTION OF MAP UNITS

Qmt Mass Movement: Talus piles composed of Castlegate Sandstone and North Horn Formation sandstones. Clast size ranges from cobbles to boulders.

Qms Mass Movement: Slope failure along bounding fault of the Gordon Creek Graben. Has been subsequently revegitated.

Qds Reclaimed land: Coal mine land that has undergone reclamation.

Qdt Coal Talus: Coal mine waste coal dump.

Qal Modern Alluvium: gravel, sand, and some clay found in the bottom of stream channels. When dry light tan in color, when wet sark tan in color.

Qal1 Alluvial Flood Plain: First level of teraces composed of reworked Bluegate Shale from the Mancos Formation. Some paleosols can be found in this terrace, and are distigusehd by there red coloring.

Qal2 Alluvial Flood Plain 2: Second level of teraces composed of reworkded Bluegate Shale from the Mancos Formation. These teraces are ~ 3 m above current stream level.

Ti Igneous Dikes: Tertiary in age composed of minette and olivine nephelinte lava. These units tend to run in a north north west direction.

Tped Pediments: These units are Tertiary in age and are cored with Mancos Shale. The outer surface is comprised of cobbles and boulders of Star Point Sandstone and Blackhawk Formation. These structures have a general dip opposite the regional dip, and dip to the east.

KTn North Horn: Tertiary in age. This unit is brown to red brown color, and is composed of mudstones and siltstones with some sandstores and marls present. This unit is 60 m thick, and is the capping unit on the Wasatch Plateau.

Kpr Price River: Late Cretaceous in age. This unit is red to brown in color and has a grain size that ranges from fine sand size particles to medium grained sands. It is composed mainly of sandstones, but does have some mudstones.

Kpc Castlegate: Late Cretaceous in age. This unit appears to be red-orange to tan in color. This unit is highly fractured in areas and is composed mainly of quartz sand grains. The bedding structures suggest that this unit was deposited mainly as upper shoreface sands and fluvial sands probably feeding the prograding deltas further to the east. Thickness of this unit is about 120 m.

Kb Blackhawk Formation: Late Cretaceous in age. This unit contains the mineable coal in the quadrangle. Coal beds out crops are 2m thick. Blackhawk formation represents depositional enviroment from lagonal coal swaps to middle shore face sandstones. The marine sandstone is tan while the beach sands are white, due to hydrocarbon bleaching. Average thickness of the formation is 100 m.

Kbs Star Point Sandstone: Cretaceous in age. This unit has three large sandstone bodies that are encased in gray to blue-gray shales. The sands are mainly quartz in composition. The individual sand bodies pinch and swell through out the quadrangle. The average thickness of this unit is 120 m. The bedding suggests that this unit was deposited in deep marine to upper shoreface environments. Some of the lower shorefaces have ophiamorpha trace fossils.

Kmbl Mancos Bluegate: Cretaceous in age. Gray to Blue-gray in color. This unit is very friable shale with very fine grains. This unit has some sand lenses that are composed of very fine sand. The overall appearance of this unit is massive in nature, and non-resistive.

Kme Emery Sandstone: Cretaceous in age. Mainly quartz sand that is tan in color surrounded by the Mancos Shale. Where the Emery outcrops it forms the lower canyons in the quadrangle. The Emery is 30 m thick with some pinching and swelling of the unit. The sand shows bedforms that indicate it was deposited as a turbidite composed of the C and D units, and shows some reworking of the sands buring storm events.

Geologic Map of the Wattis Quadrangle, Carbon and Emery Counties, Utah

by

David O. Alderks and Matt Young

Department of Geology, Brigham Young University

in cooperation with

Utah Geologic Survey
1594 West North Temple, Suite 3110
Box 146100
Salt Lake City, Utah 84114-6100

The following are gratefully acknowledged for assisting in the preparation of this map:

Bob Biek, Grant Willis, Utah Geological Survey
James Eddelman, Daniel Martin, Thomas H. Morris, Andrew Stanton, Brigham Young University, Provo, Utah
Department of Geology. Brigham Young University. Provo, Utah

MAP SYMBOLS

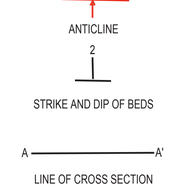

Cross Sections